Segregation in binary alloys : a LEIS study of a vicinal PtRh single crystal

Nelis, M.E.T.

Award date:
1999

Segregation in binary alloys

A LEIS study of a vicinal PtRh single crystal

Mischa Nelis February 1999

Eindhoven University of Technology
Department of Physics
Solid State Physics Division
Physics of Surfaces and Interfaces

Coached by: Ir. B. Moest
Dr. A.W. Denier van der Gon

Groupleader: Prof.Dr. H.H. Brongersma

Abstract.

The studied system is a $Pt_{50}Rh_{50}$ (611) single crystal with double atomic height steps. The segregation of this crystal is investigated by means of Low-Energy-Ion-Scattering. Since the atoms of both metals are almost of the same size we expect that strain effects, compared to the lowering of total bonding energy, play a minor role in surface segregation in PtRh crystals
The temperature influence on the surface and step composition of this crystal is investigated and also the influence of Oxygen absorption on the segregation in this crystal.
From these experiments it followed that the Platinum concentration of a $Pt_{50}Rh_{50}$ (611) crystal at room temperature is 83 ± 3 %. When the crystal is heated this concentration remains constant up to 600 degrees Celsius and than decreases to 65 % at 1000 degrees Celsius. The broken bond model with zero interaction coefficient model can not explain this behaviour, contrary to the model with a non-zero interaction coefficient of 15.5 kJ/mol together with a segregation energy of 2 kJ/mol. The Platinum concentration of a $Pt_{25}Rh_{75}$ (410) crystal, investigated by Moest et al [5], can however be well described with the broken bond model.
The Platinum enrichment at the surface can be understood when the surface free energies are looked upon. The surface energy of Platinum is lower then the surface energy of Rhodium. Therefore Platinum preferentially occupies the surface.

From the difference between the angle of incidence in the step-up and step-down geometry necessary for neighbour focussing, a miscut of the crystal of 10 degrees is extracted. This is not in accordance with the miscut of a (611) crystal, but can be explained by a small tilt of the crystal with respect to the horizontal plane.

By using small angles of incidence in the step-up direction it is possible to measure the composition of the step-edge atoms as the incident ions "slide" over the surface and only scatter from the step-edge atoms or the second layer atoms in the double height atomic steps.
The experiments show that the Platinum concentration at room temperature is in the range between 88 and 92 %. It remains constant up to 440 degrees Celsius and then decreases to 82 % at 700 degrees Celsius. This concentration is a lower limit to the real step-edge composition, since less than 100 % of the measured particles have scattered from the step-edge sites and assuming that the composition of the second layer atoms in the steps is equal to the terrace composition. The experiments are in agreement with experiments done by Moest et al [5], which also show more Platinum enrichment in the step-edges of a PtRh(410) crystal.

The crystal then has been exposed to Oxygen during 45 minutes with a pressure of

$3 \cdot 10^{-7}$ mbar. It can be seen that Oxygen is absorbed on the surface. Both the Rhodium and Platinum yield in the EARISS spectrum decrease. The Rhodium yield decreases less with respect to the Platinum yield. This could be due to Rhodium segregation but it is also possible that Oxygen preferentially absorbs on Platinum.
When it would be possible to remove the Oxygen at low temperatures the real surface composition can be obtained, for at low temperatures the mobility of the atoms is too low to reach equilibrium.
Therefore the crystal has been exposed to Hydrogen during 30 minutes at room temperature with a pressure of $2 \cdot 10^{-7}$ mbar. In the EARISS spectrum it can be seen that the Oxygen yield decreases with about 50 %. It can thus be concluded that Oxygen is not entirely removed from the surface. The Rhodium peak increases with respect to the Platinum peak. From this it can be concluded that Rhodium segregates to the surface due to Oxygen absorption.
There have to be done more experiments investigating Oxygen absorption in order to gain more insight and to be able to quantify the effect of Rhodium segregation due to Oxygen absorption.
In future work it is recommendable to expose the crystal to Hydrogen after Oxygen absorption at a temperature of, for instance, 200 degrees Celsius. This in order to remove the Oxygen entirely from the surface while maintaining the surface composition as the mobility of the atoms at these temperatures is too low to reach equilibrium.

Contents.

Chapter 1 Introduction.

The alloy PtRh is a frequently used catalyst in the automobile industry. From a fundamental point of view PtRh is interesting since it does not show complete segregation, resulting in a difference between terrace and step composition. By comparing these two compositions we hope to gain more knowledge about surface segregation. Since the atoms of both metals are almost of the same size we expect that strain effects, compared to the lowering of total bonding energy, play a minor role in surface segregation in PtRh crystals.
In recent years much work of PtRh alloys has been directed to the study of the surface composition. Siera et al [4] show a Platinum enrichment of the surface compared to the bulk concentration. This Platinum enrichment is also shown by Matsumoto et al [9] and Beck et al [11]. Siera et al also show that equilibrium at the surface at a certain temperature is reached sooner if the crystal is cooled from high temperatures to this temperature than when it is heated from room temperature.
Florencio et al [7] showed in their experiments that the surface layer is Platinum enriched while the second layer is Rhodium enriched with respect to the bulk concentration. The Platinum concentration in deeper lying layers oscillates to the bulk concentration.
Wouda et al [6] found an enhanced Platinum concentration of the step-edges on a vicinal single crystal compared to the Platinum concentration of the terrace.

We investigated the surface and step composition of a $Pt_{50}Rh_{50}$ (611) single crystal with double atomic height steps in order to get more insight in the segregation behaviour in these crystals. This was done by means of Low-Energy-Ion-Scattering. The temperature influence on the surface and step composition of this crystal is investigated. The results of these experiments are compared with those obtained on a $Pt_{25}Rh_{75}$ (410) crystal by Moest et al [5]. The results from Moest et al indicate that at room temperature the surface is Platinum enriched and that this Platinum enrichment decreases with increasing temperature. They also show that it is difficult to reach equilibrium at temperatures below 400 degrees Celsius.

The influence of Oxygen adsorption on the surface composition of the surface is also investigated. Based on investigations reported by other scientists [8,9,10,11], Rhodium is expected to segregate to the surface due to Oxygen adsorption. Possible preferential adsorption of Oxygen on either Platinum or Rhodium complicates these investigations. Preferential absorption would result in the shielding of either Platinum or Rhodium atoms when Oxygen is adsorbed on either of them. Experiments done by van Delft et al [10] show preferential absorption of Oxygen on Rhodium.

In Chapter 2 the principles of Low-Energy-Ion-Scattering and segregation will be discussed, after which in Chapter 3 the used experimental techniques and setup will be described. The results are presented and discussed in Chapter 4. The conclusions will be given in Chapter 5

Chapter 2 Theory.

2.1 Introduction.

In this chapter the principles of Low-Energy-Ion-Scattering and segregation in binary alloys will be discussed. In section 2.2 therefore ion-atom interactions will be discussed and in section 2.3 segregation in binary alloys.

2.2 Ion-atom interactions.

2.2.1 Laws of momentum and energy conservation.

According to Bohr (1948) the interaction of medium and low energy particles with a surface can be expressed as if the target particle in the surface is a free particle. In Figure 2.1 a scattering scheme of two colliding particles is shown.

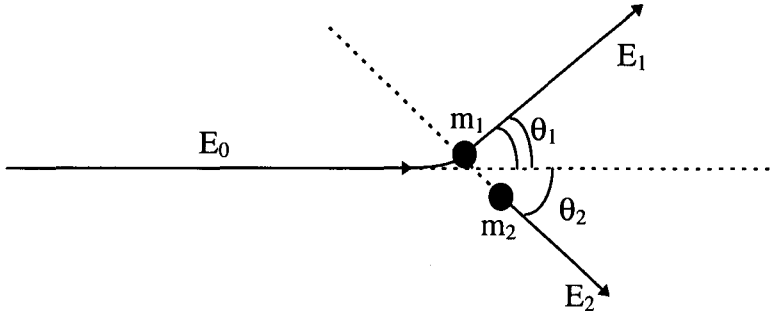

Figure 2.1 Scattering scheme of two colliding particles.

An ion of mass m_1 moves with an energy E_0 with respect to a fixed target atom of mass m_2. When these two particles collide, the moving ion will be deflected from the initial direction by an angle θ_1 and will have an energy E_1, while the target atom will deflect by an angle θ_2 relative to the initial ion motion and acquire an energy E_2. This target atom is also called the recoil atom. Starting from the momentum and energy conservation laws and when only considering elastic collisions it can be shown [1] that the ion will have an energy E_1 of:

$$E_1 = \frac{E_0}{(1+\mu)^2}(\cos\theta_1 \pm \sqrt{\mu^2 - \sin^2\theta_1})^2 \qquad (1)$$

with $\mu=m_2/m_1$.

The recoil atom will have an energy of:

$$E_2 = \frac{4\mu}{(1+\mu)^2} E_0 \cos^2 \theta_2. \qquad (2)$$

So both energies are dependent of μ. When the identity of the incident ion is known and when the energy of either the ion or the recoil particle is measured, the target particle can be identified.

2.2.2 Neutralization.

The neutralization probability of noble gas ions in a collision is very high, often even more then 95%. This means that when an incident ion penetrates into the bulk instead of scattering back from the first layer it is more then likely that the ion will be neutralized. When therefore noble gas is used to bombard a sample and only the energies of the scattered ions are measured, knowledge is obtained about the surface.

2.2.3 Shadowing, blocking and focusing.

When an ion passes an atom it will be deflected due to the Coulomb interaction. So behind the target atom there is a ion free region. This region is called the shadow cone (see Figure 2.2).

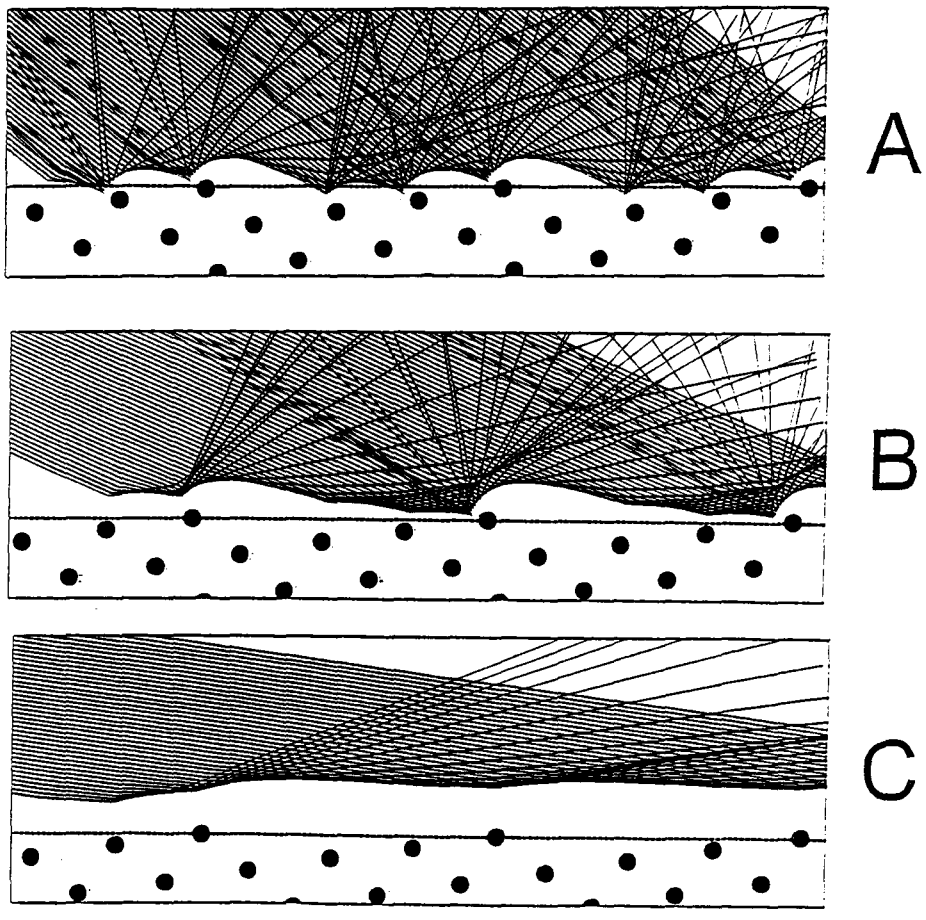

Figure 2.2 Example of neighbour focusing (a), the "sliding" effect (b) and the mirror reflection mode (c).

The atoms in the shadow cone are not visible to an incident ion beam. This is called shadowing. It is also possible that the shadow cone prevents a scattered ion to enter a detector. This is called blocking.
Martynenko (1964) showed that on the edge of the shadow cone the intensity of the flux exceeds that of the undistorted flux by ±10%. So the ions are "focused" on the edge of the shadow cone. This is called focusing. An example of neighbour focusing can be seen in Figure 2.2a. As can be seen in this figure the incoming ions are focused on neighbouring atoms.
At smaller angles of incidence the incoming ions start "sliding" over the surface due to the potentials of all surface atoms. This implicates that the incoming atoms slide over the surface and then scatter of either a step-edge atom or a surface defect, as can be seen in Figure 2.2b.
When a very small angle of incidence is used the surface potential formed by all the surface atoms is very smooth and therefore reflects the incoming ions as a mirror. The flux of scattered ions is concentrated around the same angle as the angle of incidence. This is called the "mirror reflection mode". This is shown in Figure 2.2c.

2.3 Segregation.

2.3.1 Introduction.

Minimizing the total energy of the crystal is the driving force of segregation of atoms to the surface. Segregation to the surface is different from the segregation between two bulk phases because of the finite depth of the surface region. Segregation in binary alloys is discussed.
The following assumptions are made:

- The crystal is a closed system consisting of the two open systems bulk and surface.
- The bulk phase is infinite and the surface phase is finite in size.
- Atoms can be exchanged between these two phases until the total energy is minimized.

For a closed system of two phases, when pressure and temperature are equal for both phases, the system minimizes the Gibbs free energy G.
This Gibbs free energy can be written as [2]:

$$G = G^B + \sigma s = n_1^\phi \mu_1^\phi + n_2^\phi \mu_2^\phi + n_1^B \mu_1^B + n_2^B \mu_2^B , \qquad (3)$$

where σs may be viewed as the surface energy (σ = surface tension and s = surface area), G^B is the Gibbs free energy of the bulk, n_i the number of moles present of species i and μ the chemical potential. The superscript indicates the relevant phase: ϕ is the surface and B is the bulk.
From the assumptions that the segregation will not change the bulk concentration and the chemical potential terms μ_i^B in the bulk remain constant it can be shown that:

$$\sigma s = n_1^\phi (\mu_1^\phi - \mu_1^B) + n_2^\phi (\mu_2^\phi - \mu_2^B) . \qquad (4)$$

It is clear from equation (3) that the condition for equilibrium for a constant surface area s and constant G_B is:

$$\frac{\partial \sigma}{\partial n_i^\phi} = 0 , \qquad (5)$$

i.e. the surface will be in equilibrium with the bulk when the surface tension σ is a minimum.
When equation (4) is substituted in equation (3) and with the well known Gibbs Duhem relation $\sum n_i^\phi \, \partial \mu_i^\phi / \partial n_i^\phi = 0$ this leads to:

$$\mu_1^\phi - \mu_1^B - \mu_2^\phi + \mu_2^B = 0 . \qquad (6)$$

The chemical potentials μ_1^{ν} and μ_2^{ν} can be written by means of a regular solution model (see for a full discussion [2]) as:

$$\begin{aligned} \mu_1^{\nu} &= \mu_1^{0\nu} + \Omega_{12}(C_2^{\nu})^2 + RT \ln C_1^{\nu} \\ \mu_2^{\nu} &= \mu_2^{0\nu} + \Omega_{12}(C_1^{\nu})^2 + RT \ln C_2^{\nu} \end{aligned} \tag{7}$$

where ν indicates the relevant phase ϕ or B and Ω_{12} the interaction parameter given by:

$$\Omega_{12} = Z\omega_{AB}N_0 . \tag{8}$$

Z is the number of nearest neighbours in the bulk, N_0 the constant of Avogadro and $\omega = u_{AB} - 1/2(u_{AA} + u_{BB})$. The energy $u_{\alpha\beta}$ is associated with the pair interaction between atoms of species α and β.
When the surface concentration of a compound of a binary alloy, $C_{s,1}$, is written as n_i^{ν}/n, with n the total number of moles present, it can be shown that in equilibrium $C_{s,1}$ can be expressed as [2]:

$$\frac{C_{S,1}}{1 - C_{S,1}} = \frac{C_{B,1}}{1 - C_{B,1}} \exp\left(\frac{\Delta G + 2\Omega_{12}(C_{S,1} - C_{B,1})}{RT}\right) \tag{9}$$

where $\Delta G = \mu_1^{0,B} - \mu_1^{0,S} - \mu_2^{0,B} + \mu_2^{0,S}$ is the segregation energy. The term $\mu_i^{0,\alpha}$ is the standard chemical potential for compound i and phase α.
Equation (9) is known as the Bragg-Williams expression.
By using equations (4) and (7) the surface tension can also be expanded in terms of interaction parameters, but that is too cumbersome to repeat here.
Two cases can be distinguished: a zero and a non-zero interaction coefficient.

2.3.2 Zero interaction coefficient ($\Omega_{12} = 0$).

A zero interaction coefficient leads to:

$$\frac{C_{S,1}}{1 - C_{S,1}} = \frac{C_{B,1}}{1 - C_{B,1}} \exp\left(\frac{\Delta G}{RT}\right). \tag{10}$$

The expression with zero interaction coefficient is known as the Langmuir-McLean expression
The segregation energy ΔG with a zero interaction coefficient can also be written as $\Delta G = \Delta H_{sub} * N/N_{tot}$, where N is the number of broken bonds at a certain site, N_{tot} the total number of bonds and ΔH_{sub} an approximation of the sublimation energy. This is called the broken bond model.

In Figure 2.3 the surface coverage of compound 1 is shown for $C_{B,1}$=0.0005, ΔG=40 kJ/mol and a zero interaction coefficient. As can be seen in Figure 2.3 the surface concentration first stays constant and then decreases to the bulk value.

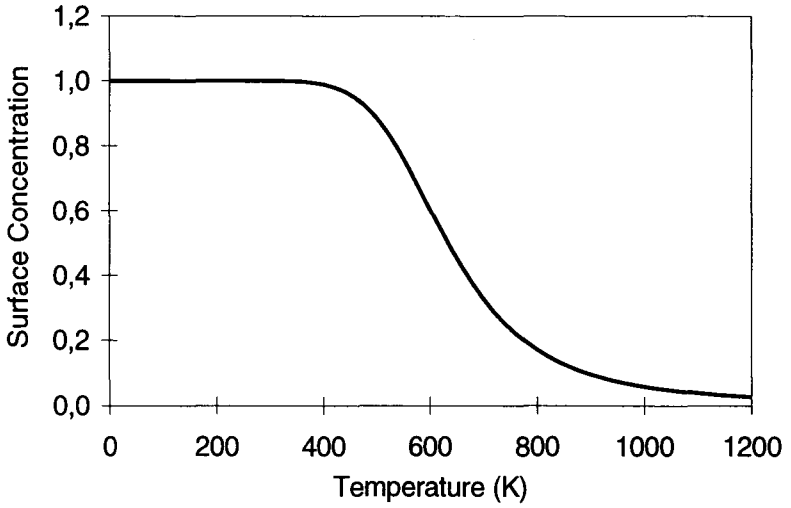

Figure 2.3 Surface coverage versus temperature calculated from equation (10) for $C_{B,1}$=0.0005, ΔG=40 kJ/mol and Ω_{12}=0.

In Figure 2.4 the surface coverage of compound 1 is shown for $C_{B,1}$=0.5, ΔG=2 kJ/mol and a zero interaction coefficient. The surface concentration at low temperatures is 1 and then also decreases to the bulk value.

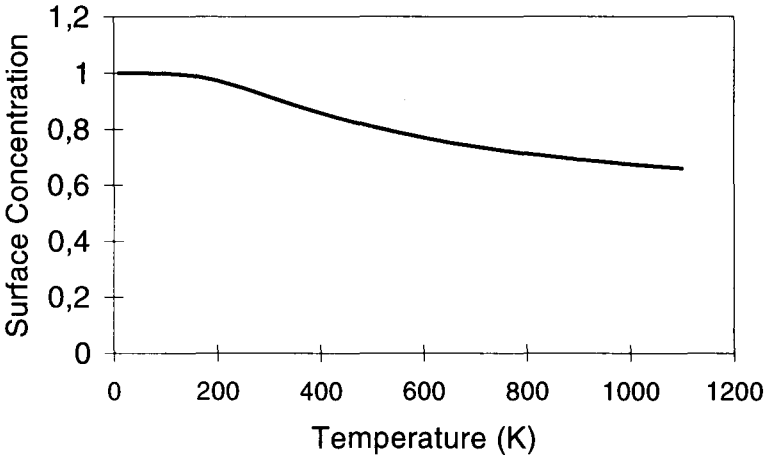

Figure 2.4 Surface coverage versus temperature calculated from equation (10) for $C_{B,1}$=0.5, ΔG=6 kJ/mol and Ω_{12}=0.

2.3.3 Non zero interaction coefficient ($\Omega_{12} \neq 0$).

A non zero interaction coefficient gives:

$$\frac{C_{S,1}}{1-C_{S,1}} = \frac{C_{B,1}}{1-C_{B,1}} \exp\left(\frac{\Delta G + 2\Omega_{12}(C_{S,1} - C_{B,1})}{RT}\right). \qquad (11)$$

The interaction coefficient may be either positive (attractive) or negative (repulsive). Two cases can be distinguished: a low bulk concentration and a high bulk concentration.

Low bulk concentration.
First the case of low bulk concentration will be discussed.
In Figure 2.5 the surface coverage is plotted against temperature with values $C_{B,1}$=0.0005, ΔG=20 kJ/mol and Ω=18 kJ/mol. Indicated in this figure is a hysteresis effect.

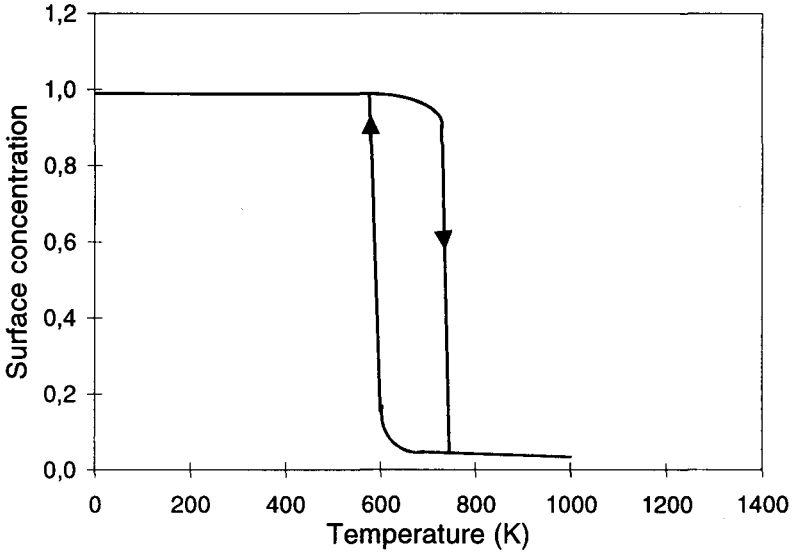

Figure 2.5 Surface coverage versus temperature for $C_{B,1}$=0.0005, ΔG=20 kJ/mol and Ω_{12}=18 kJ/mol.

This hysteresis effect can be explained with the surface tension σ. Equation (11) was obtained by the condition that $\partial\sigma/\partial n_i = \partial\sigma/\partial C_{S,1} = 0$. The solutions therefore correspond to either a maximum or a minimum in the surface tension. Only the minimums are stable solutions.
In Figure 2.6 the surface tension as calculated with equations (4) and (7) is plotted against $C_{B,1}$ [2].

At a temperature of 500 K the system is in a state of high surface concentration (the minimum on the right hand side). When now the temperature is increased the transition from high to low surface concentration occurs when the barrier in the middle has disappeared. So at a temperature of about 650 K the system abruptly moves from high coverage to low coverage.
When starting at high temperatures like 700 K the system is in a state of low surface concentration (the minimum on the left hand side). When the temperature is decreased the transition from low to high surface concentration occurs at a temperature of about 550 K. This explains the hysteresis effect.

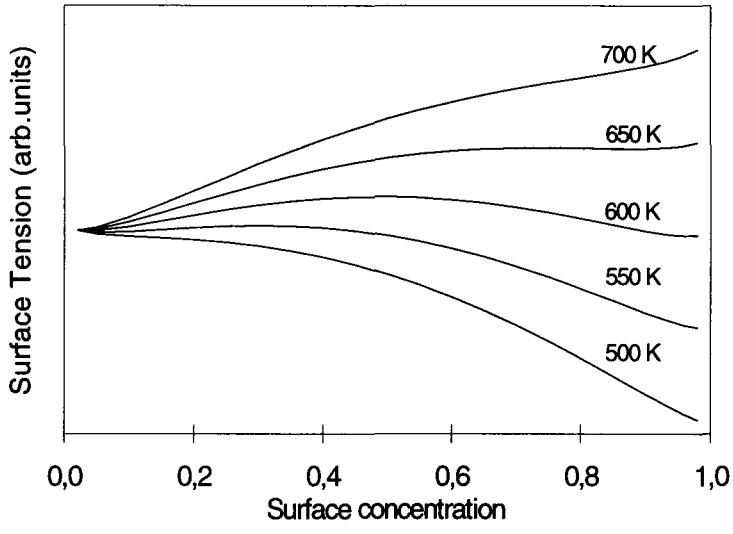

Figure 2.5 Surface tension versus surface concentration for $C_{B,1}$=0.0005, ΔG=20 KJ/mol and Ω_{12}=18 KJ/mol.

High bulk concentration.
Now the case of a high bulk concentration is looked at.
In Figure 2.6 the surface coverage is plotted against temperature with values $C_{B,1}$=0.5, ΔG=2 kJ/mol and Ω=15.5 kJ/mol.

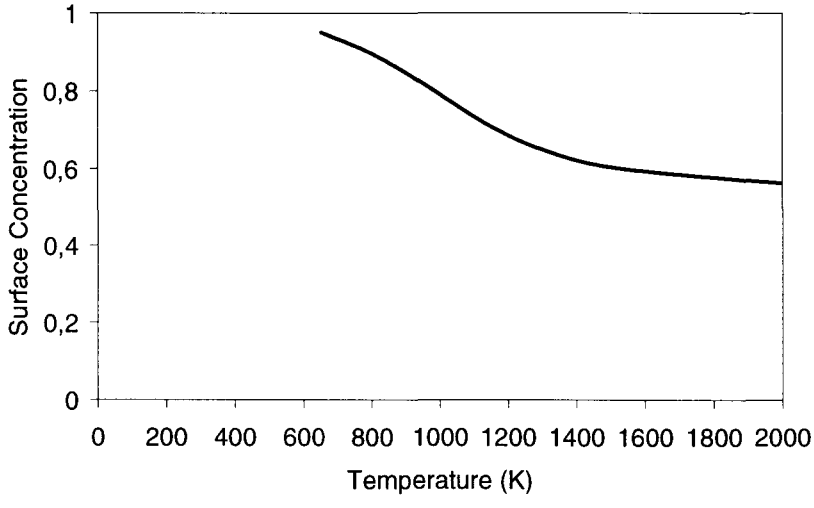

Figure 2.6 Surface coverage versus temperature for $C_{B,1}$=0.5, ΔG=2 kJ/mol and Ω_{12}=15.5 kJ/mol.

As can be seen in Figure 2.6 the hysteresis effect has disappeared. This can be explained again with the surface tension as plotted in Figure 2.7.

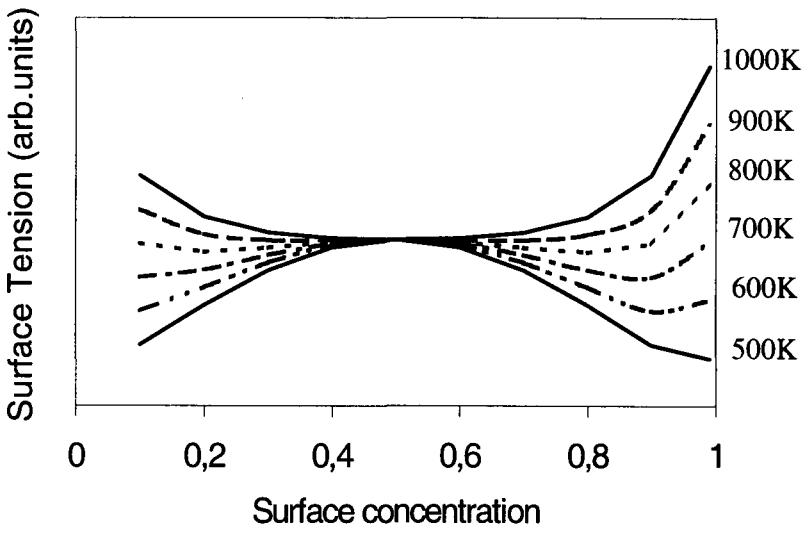

Figure 2.7 Surface tension versus surface concentration for $C_{B,1}$=0.5, ΔG=2 kJ/mol and Ω_{12}=15.5 kJ/mol.

When the temperature is increased starting at 600 K the surface concentration stays at the minimum of the surface tension with a surface concentration of 0.9, until about 700 K. The surface concentration then starts to move to the minimum at 0.5. From this Figure 2.7 it is clear hat no hysteresis effect occurs.
It can therefore be concluded that in the case of a high bulk concentration as 0.5 no hysteresis effect occurs.

Chapter 3 Experimental set-up.

3.1 Introduction.

In Low-Energy-Ion-Scattering (LEIS) noble gas ions are used to bombard a surface, where they will have binary collisions with the surface atoms. The energy of these scattered ions is directly related to the mass of the target atoms. The total yield at a certain energy is a measure for the concentration of that particular element at the surface.
LEIS has to be done in ultra high vacuum (UHV) because else the surface of the sample is contaminated before any measurements can be done. This is the reason that in the main chamber the pressure is about 10^{-9} mbar.
In figure 3.1 a general overview of the used main chamber is shown.

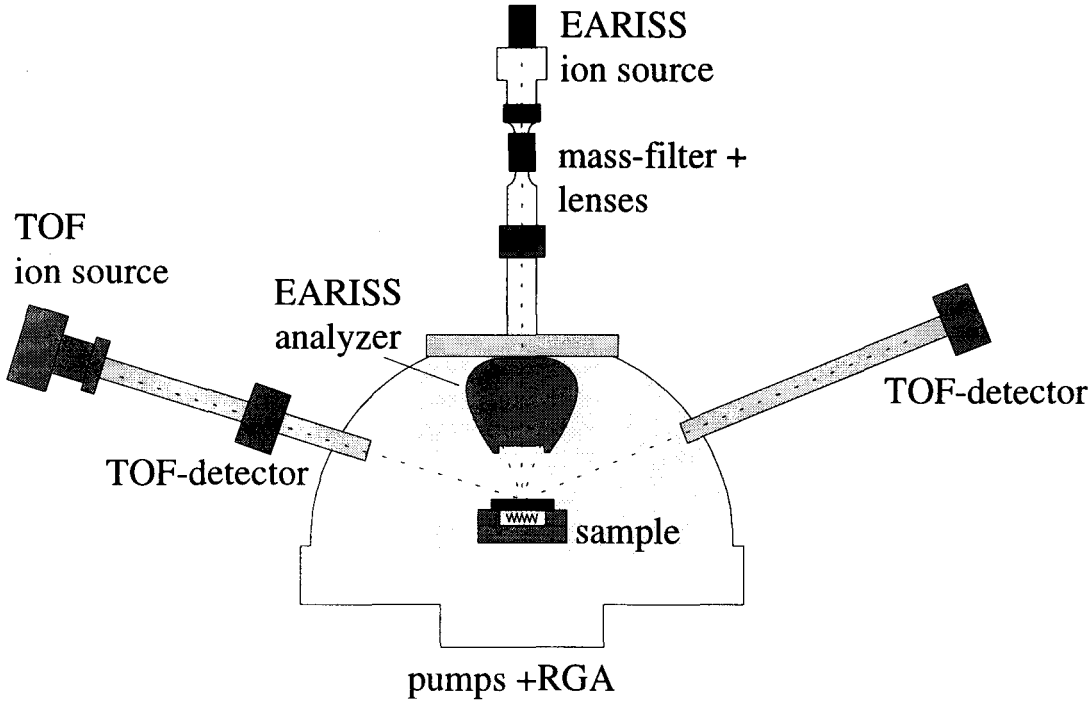

Figure 3.1 General overview of the main vacuum chamber.

The surface of the sample is cleaned by bombarding the surface of the sample with Ar^+-ions. This is called sputtering. The Ar^+-ions are created with an ion source, with an energy of 0.5-5 keV. In this way atoms and with them any contaminants are removed from the surface of the sample.
The sample is heated with an oven which is made of a thin Tantalum wire. At elevated temperatures electrons are emitted from this wire. By supplying a high negative voltage to this oven these electrons are accelerated towards the sample. This is called e-beam heating.

The temperature of the sample is measured with a CHINO comet 1000 pyrometer with an absolute accuracy of ±50 degrees Celsius and a reproducibility within ±10 degrees Celsius. The lower limit of this pyrometer is 400 degrees Celsius. Below this temperature the power through the oven is measured and this is used as an indication for the temperature.
By heating the sample very quickly to high temperatures the structure of the surface will reconstruct. This can be verified with LEED (Low Energy Electron Diffraction). Connected to the main chamber there is a LEED-chamber. The pressure in this chamber is about 10^{-10} mbar. For more detailed information about LEED see [3].
Also connected to the main chamber is a storage chamber in which 6 samples can be kept in vacuum.
In the main chamber the sample is placed in a manipulator, which has 6 degrees of freedom.
In this main chamber LEIS can be performed in two different ways: using the EARISS detector on one side and on the other side using the Time-Of-Flight technique. In section 3.2 the EARISS detector will be further explained and in section 3.3 the Time-Of-Flight-technique. The investigated crystal will be described in section 3.4.

3.2 The EARISS.

The name EARISS stands for Energy and Angle Resolved Ion Scattering Spectrometer. This is a detector which, as the name does suspect, produces an energy and angle dependent signal.
In figure 3.2 the used set-up is shown.

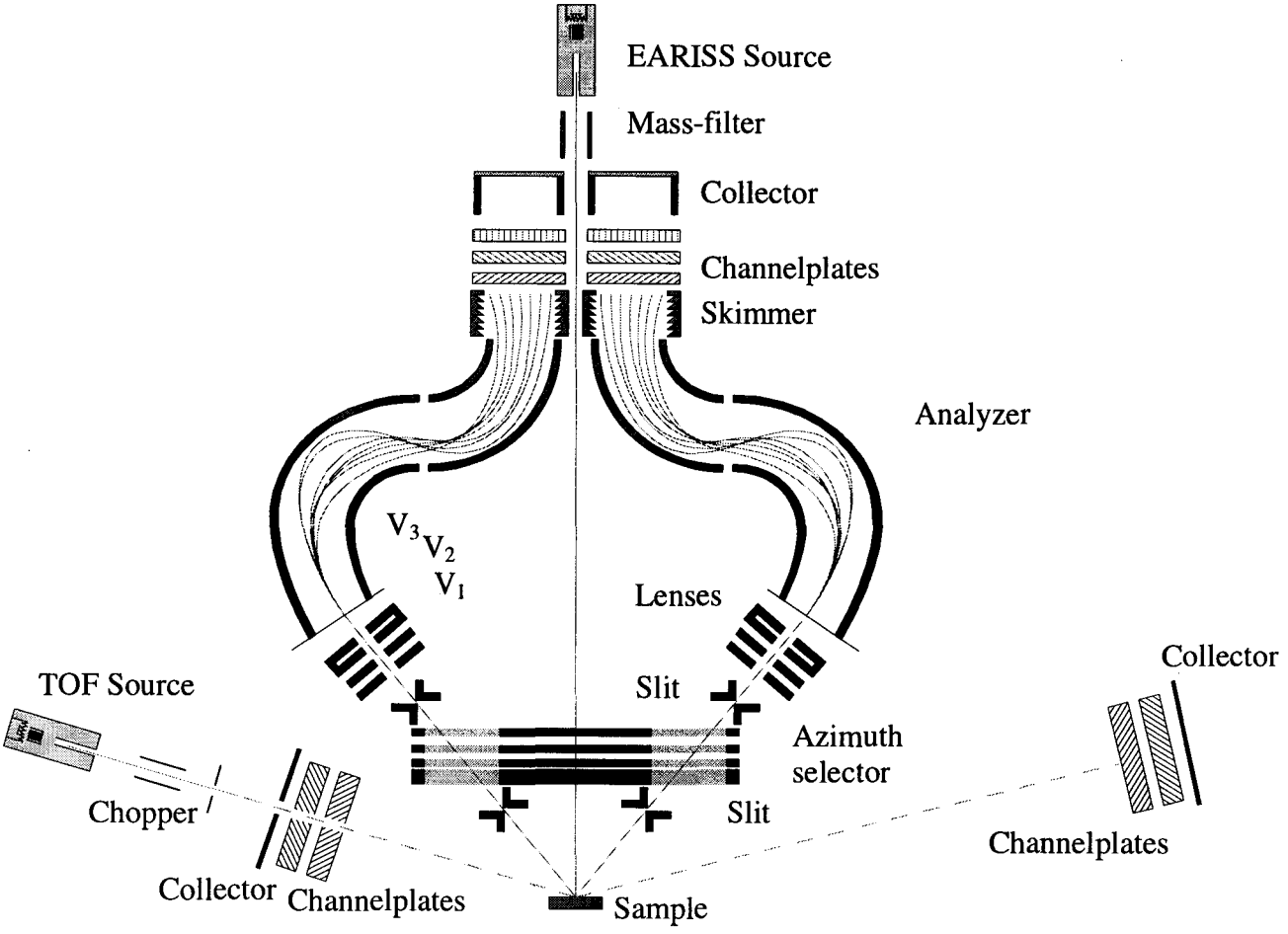

Figure 3.2 The set-up of the EARISS.

The ions are produced in the ion source in top of the set-up and are accelerated to an energy up to 5 keV. They collide with the sample in the bottom of the set-up. The slits select the ions which are backscattered with an angle of 145°. Ions backscattered with an angle of 145° but with a nonzero angular momentum give rise to a decreasing angle resolution. The azimuth selector therefore selects only those ions with zero angular momentum. The beam of the remaining ions is then focused by lenses V1 and V2. The ions are accelerated by lens V3 and enter the analyzer which consists of rotation symmetric plates. High voltage is supplied to these plates and by doing so only those ions with an energy of $E=E_{pass} \pm 5\%$ are able to pass through this analyzer and reach the detector. In order to have a good resolution this E_{pass} has to be as small a possible. This would implicate that many measurements have to be done before the whole desired spectrum is measured and therefore damage would be done to the surface. The choice of E_{pass} depends on these two considerations. In these experiments E_{pass} =3 keV. This E_{pass} ensures a good resolution and little damage to the surface.

The detector consists of three channelplates and a collector plate. These channelplates are rotation symmetric plates pierced by many small channels. In the middle they have a passage for the ion beam coming from the ion source.
The channels are coated with a high resistance material with a larger secondary electron emission coefficient. These channelplates are supplied with about 800 V, with a difference of 50 V between each plate. When an ion hits the wall of a channel, electrons will be emitted and they in turn will liberate more electrons. So a cloud of electrons leaves the first channelplate. This cloud is accelerated between the first and the second plate and will be amplified in the second plate. The same thing happens in the third channelplate. The channels in the first and second channelplate are not parallel to the beam and each other in order to create a larger emission of electrons. The cloud of electrons which leaves the third channelplate will grow larger in the "driftspace" and will than impinge on the collector plate.
The design of this plate enables the determination of the position and the energy of the ion.

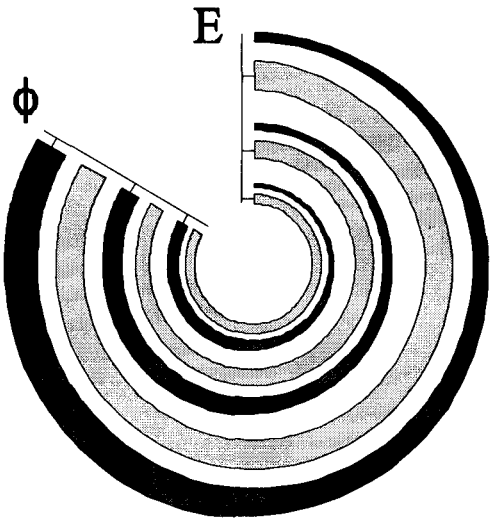

Figure 3.3 The collector plate design of the EARISS detector.

The collector contains two types of stripes, the E- and the Φ-stripes (see Figure 3.3). The E-stripes have a constant width in the Φ direction, but get wider towards the outside of the plate. Ions with a high energy (so E_{pass}+5%) will impinge on the outer region of the first channelplate. The emitted electron cloud will therefore also impinge on the outer region of the collector plate. The number of collected electrons on this E-stripe will be larger then when the cloud would have hit the inner region of the collector plate and thus a smaller E-stripe. Because the electron clouds will be different in size the signal is divided by the total charge Q_{tot}. This Q_{tot} is determined by measuring the drop in voltage over the last channelplate when the cloud of electrons leaves this last channelplate. By following this procedure the energy of the ion is determined.
The Φ-stripes widen as a function of Φ itself, while they remain constant in width as a function of radius. So the received signal on the Φ-stripes divided by Q_{tot} is a function of Φ.

The received signals are amplified together with the signal of Q_{tot}. The amplifiers make the signals suitable for the ADC's. The digital values of E and Φ are than divided by the value of Q_{tot} and put in a two-dimensional MCA (Multi Channel Analyzer).
The output is a 2D histogram as can be seen in Figure 3.4a. The grey-values of the graph in the histogram are proportional to the number of collected ions. If one is only interested in the yield as a function of either energy or angle, the total yield in the particular channel can be added together. These results are shown in Figure 3.4b and 3.4c.

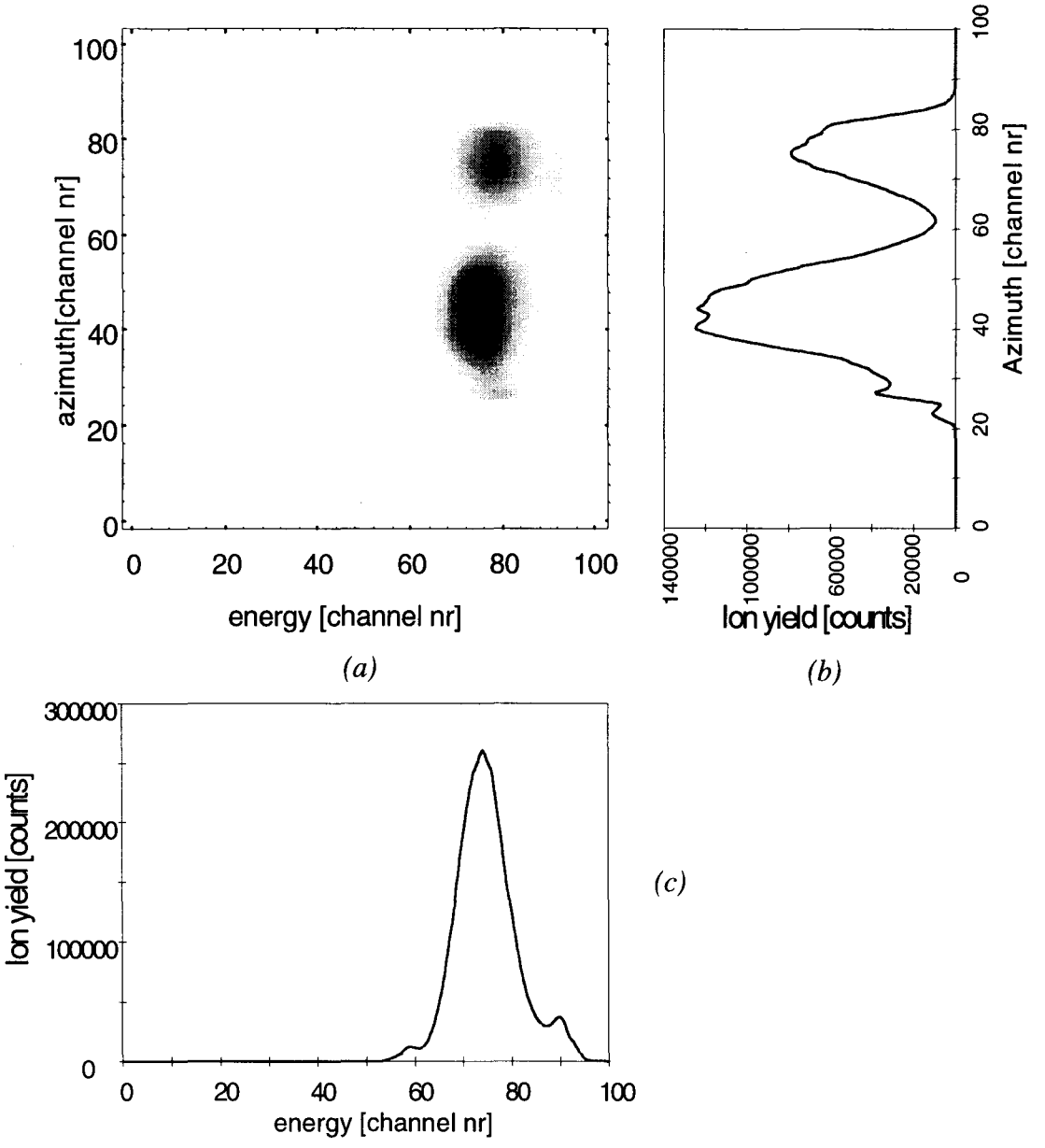

Figure 3.4 Yield as a function of : energy and azimuth (a), azimuth (b) and energy (c).

The typical error in these experiments is 5 %. This error is based on the error in the determination of the sensitivity for different elements and the statistical error involved.

3.3 The Time-Of-Flight technique.

The Time-Of-Flight (TOF) technique is very useful in analyzing the composition and structure of the surface of a surface. Forward and backward TOF can be distinguished. The difference is that forward scattering makes it possible to detect particles removed from the surface by the incoming ions, the recoil particles, while backward scattering of course only uses the backscattered projectiles, which are scattered over 180 degrees. They are complementary because with forward TOF also light elements can be detected and backward TOF has a high resolution for heavy elements. Another advantage of the backward TOF is that interpretation is relatively easy because no blocking occurs of binary collisions. This is not the case in forward TOF.
The TOF technique is quite straightforward. When a particle collides with another particle energy is transferred. When the energy of the incident particle is known, the energy of either the scattered or the recoil particle is directly related to the mass of the target particle (assuming a kinetic energy before the collision of this target particle of zero). In TOF the flight time of the particles is measured. The flight time is directly related to the energy. In this way it is possible to determine the surface composition.

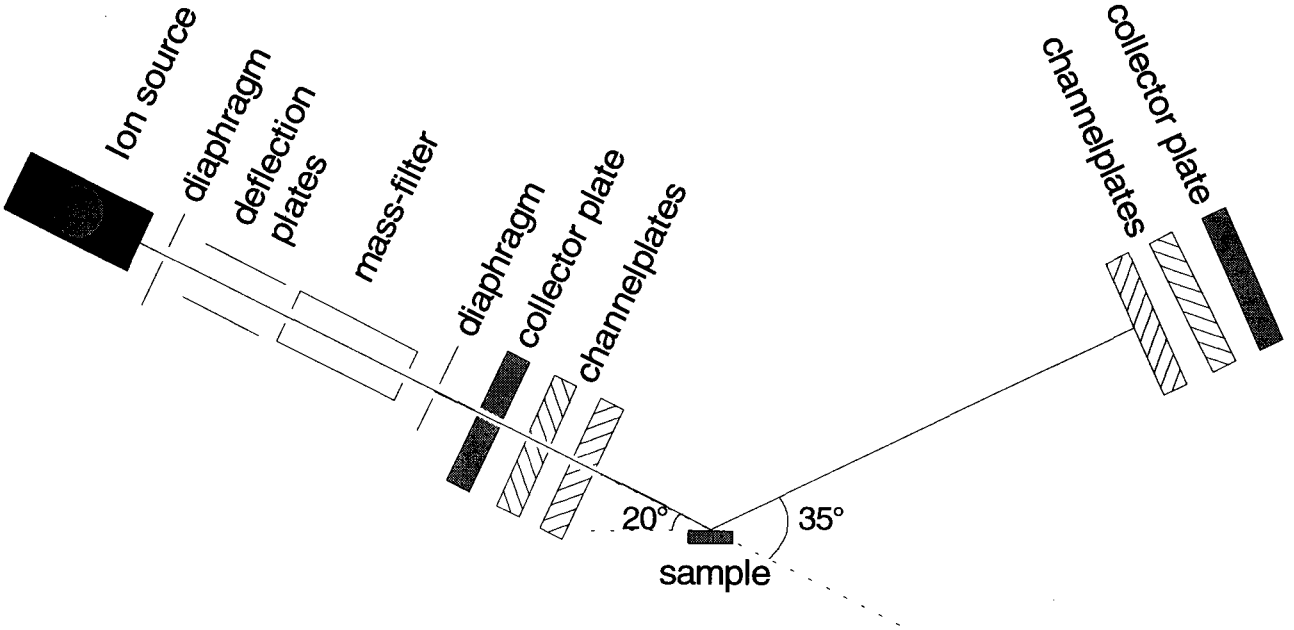

Figure 3.5 A schematic view of the Time-Of-Flight set-up.

In Figure 3.5 a schematic view of the set-up is shown. The ion source creates a constant beam of ions. This beam is chopped by switching the voltage over the deflection plates between zero and a selectable voltage between 20 and 70 V. The ions with the proper mass are selected by the mass-filter. The incident ions on the surface of the sample scatter and may reach either the forward or the backward detector. The incident particle can also remove a particle out of the surface and this recoil particle can reach the forward detector.
The detectors are based on the same principle as the EARISS detector. They consist of two channelplates and one collectorplate. The collected charge is amplified and shaped into a voltage pulse.

In forward TOF the time of flight is measured by a TAC (Time to Amplitude Converter). This TAC is triggered by the pulse generator which drives the deflection plates and is stopped by the pulse from the amplified detector signal. The voltage from the TAC is converted into a digital value with an ADC and put into a MCA.
An example of a forward TOF spectrum can be seen in Figure 3.6.

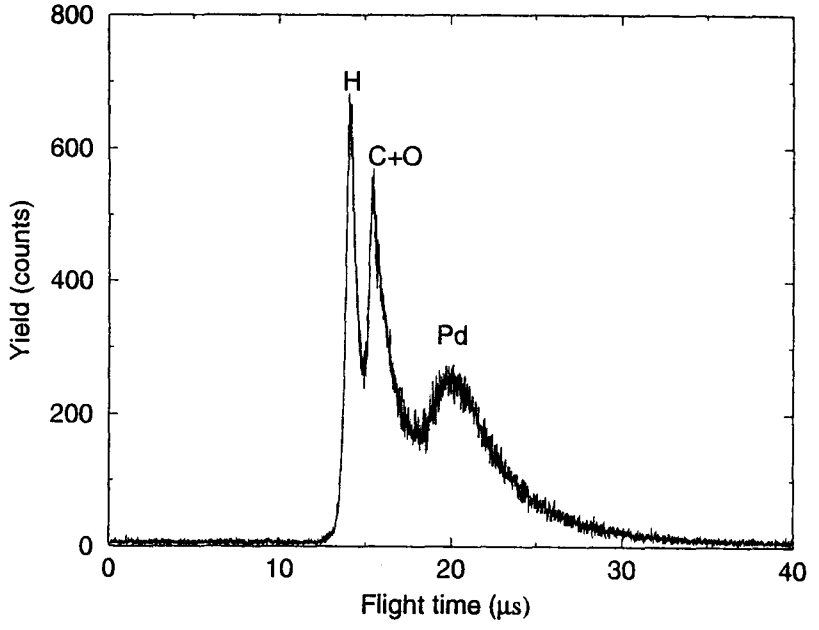

Figure 3.6 An example of a forward TOF spectrum.

The timing diagram of the backward TOF is schematically shown in Figure 3.7. The delay-time and the start pulse are triggered by the repetition generator. The frequency of the repetition generator can be varied between 2-22 kHz. The start pulse drives the deflection plates. During this pulse ions are able to pass through the deflection plates. When the delay-time has passed the register shown in Figure 3.8 receives pulses during the measuring-time and the counters, also shown in Figure 3.8, start incrementing.

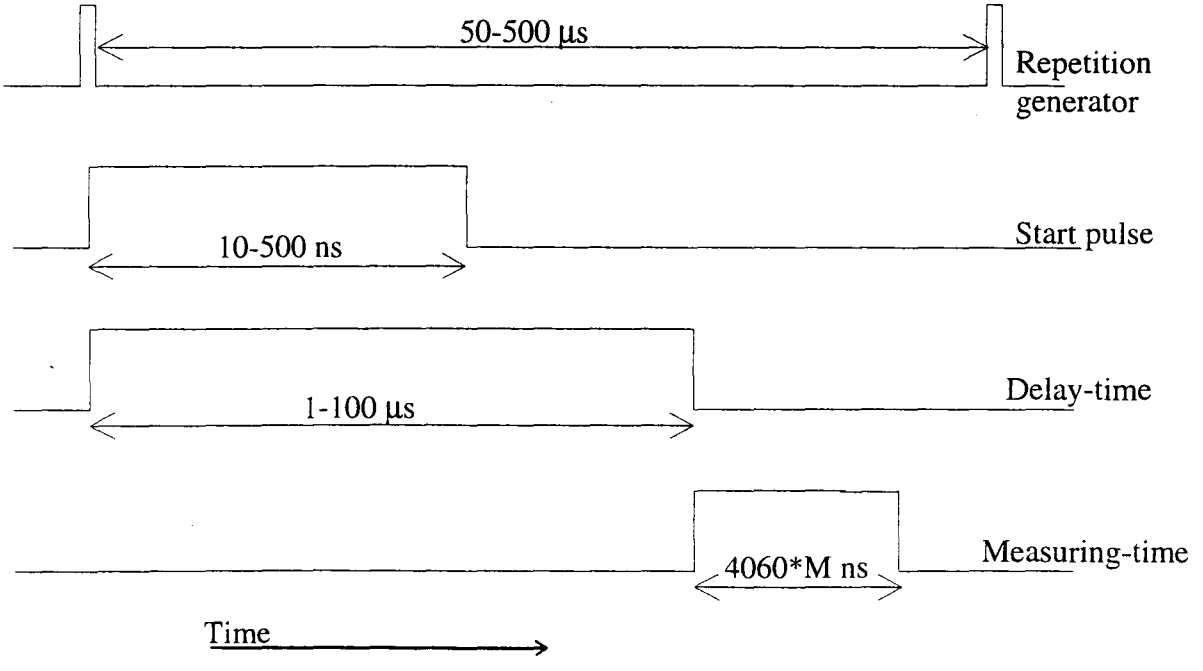

Figure 3.7 The schematic timing diagram of the backward TOF.

A schematic diagram of the electronics involved is shown in Figure 3.8. The frequency of pulses coming from the pulse generator is divided by a factor M. This factor is selectable by the user. The measuring flip-flop is also driven by the signal coming from the pulse divider and therefore the measuring time is selectable by the user (10,20,40,80,160*4060ns).
The register is driven by the measuring time flip-flop and the detector pulses. When the register receives a pulse it pushes the zero downwards and by doing this it stops the first counter with counting pulses and so on. The values in the counters can be translated to flight-times. After the measuring-time has passed the counters and pulse generator are reset. By repeating this cycle the spectrum as shown in Figure 3.9 is generated.

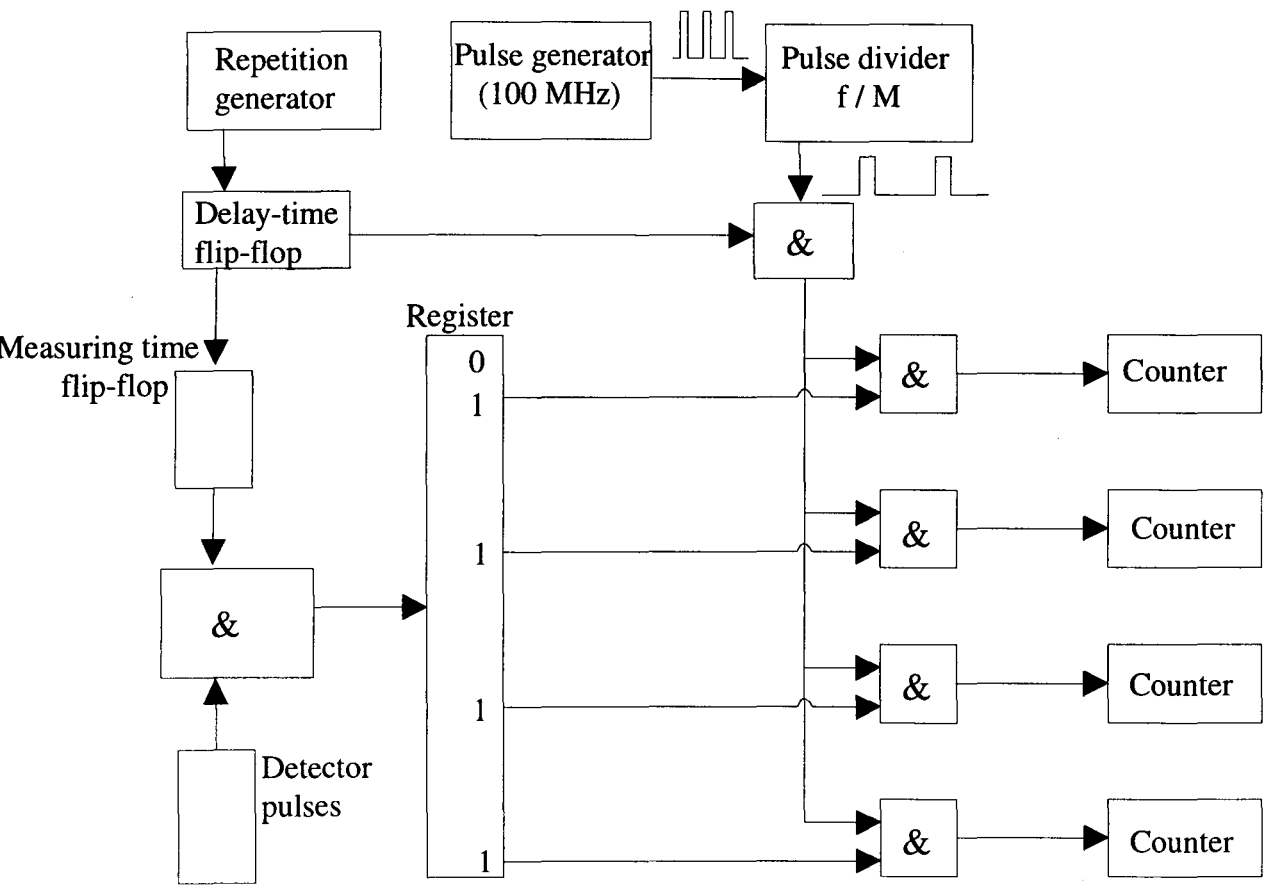

Figure 3.8 A schematic diagram of the electronics involved in backward TOF.

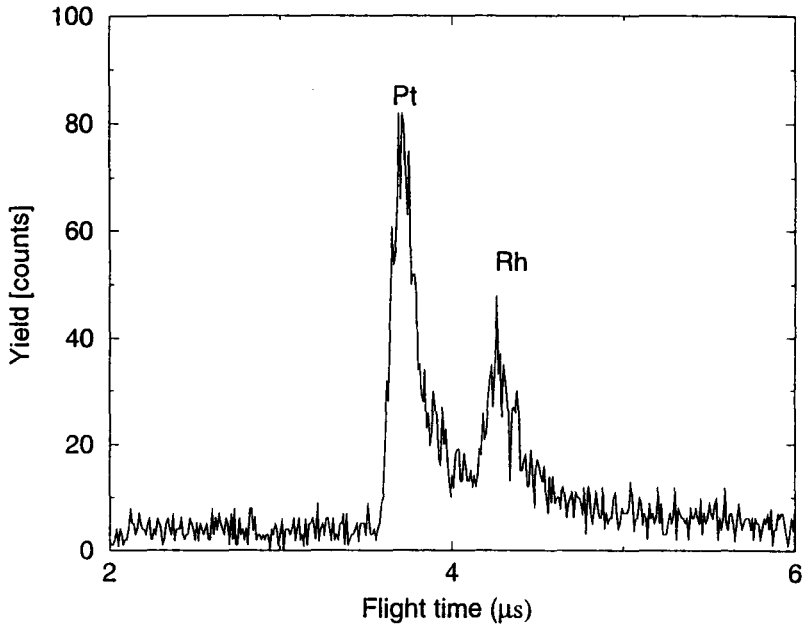

Figure 3.9 An example of a backward TOF spectrum.

The backward TOF is more efficient then forward TOF because it has 4 counters and is therefore able measure 4 ions in every cycle, instead of the 1 ion the forward TOF is able to measure.
The TOF detector measures, contrary to the EARISS detector, not only ions but also neutrals. In order to be only sensitive to the atoms in the surface it is therefore important to choose a good combination of the kind of incident ions, the energy and the incident angle.

The structure of a surface can also be investigated by using the shadowing and focussing effects.
When for instance regularly spectra are taken while turning the sample in the horizontal plane, the total yield in the peaks as a function of azimuth in the horizontal plane can be extracted. From this graph the directions of the main crystal axis can be determined, as the graph is symmetric around these directions.
When the angle of incidence is varied it is possible to focus on certain sites. When for instance a stepped surface is used, information is obtained about the composition of the step-edge sites when the beam is focused on these sites.

In these experiments the error is typically 10 %. This error is caused by the error in the determination of the detector sensitivity of different elements and the statistical error involved.

3.4 The investigated crystal.

The investigated crystal is a $Pt_{50}Rh_{50}$ (611) single crystal with double atomic height steps. A (611) crystal has a miscut of 13° and it has a FCC structure which is shown in Figure 3.7, together with the direction of the steps. The [110] directions is the step-down geometry, whereas the $[\overline{1}\overline{1}0]$ direction is the step-up geometry.

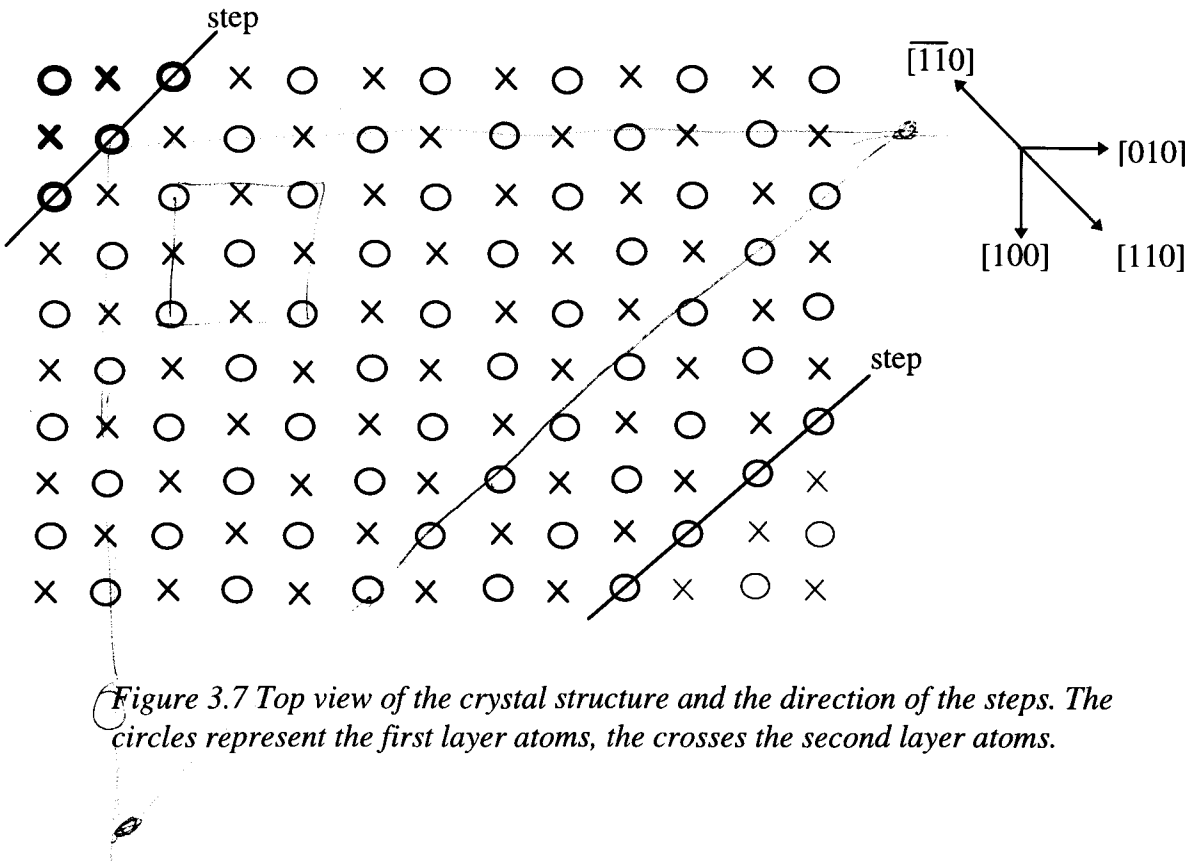

Figure 3.7 Top view of the crystal structure and the direction of the steps. The circles represent the first layer atoms, the crosses the second layer atoms.

Chapter 4 Results.

4.1 Introduction.

In section 4.2 EARISS experiments will be discussed, starting in paragraph 4.2.1 with the experiments done to extract the surface composition as a function of temperature. From these experiments a temperature can be determined at which the atoms are still mobile but not mobile enough to reach equilibrium when the temperature is rapidly decreasing. The mobility at this particular temperature is investigated in paragraph 4.2.2.
In section 4.3 backward TOF experiments in order to determine the step-edge composition as a function of temperature will be discussed. Therefore first the experiments to determine the step direction will be discussed in paragraph 4.3.1. The experiments which define the step-up direction are described in paragraph 4.3.2 and paragraph 4.3.3. Paragraph 4.3.4 finally contains the step-edge composition as a function of temperature.
In section 4.4 the introductory oxygen absorption experiments on the surface of this PtRh crystal will be described. Recommendations for future work in this field will also be given in this section.

4.2 EARISS experiments.

4.2.1 Segregation as a function of temperature.

Experimental.
In this section the temperature influence on the Platinum concentration at the surface is investigated.
The experiments are done with the EARISS detector. The spectra were taken with 2 keV Ne^+ ions. This combination of ion and energy provides a good resolution while the surface only has to be submitted to a dose of 10^{12} ions/cm^2 for obtaining the desired spectrum. This dose is below the upper limit at which the surface is damaged in such a way that it influences the results of the experiment.
The experiments were performed three times at different spots at each temperature in order to obtain better statistics. The number of counts in the peak area was determined using a fit program, which fits a Gauss to the peaks and a linear fit to the background. The total yield is the yield in the Gauss peak as calculated by the fit program.
Before each experiment the crystal was flashed three times to a temperature of 1050 degrees Celsius.
Immediately after the last flash the crystal cools down to the desired temperature. From experiments done by Siera et al [4] it is known that by doing this equilibrium is reached sooner than when the crystal is heated from room temperature. The time the crystal is given to reach equilibrium was 10 minutes above 700 degrees Celsius and 60 minutes below 700 degrees Celsius.
The sensitivity of the EARISS detector is different for different elements. This is among others due to the difference in crossection. In order to correct for this sensitivity reference samples were used. The used samples were a Pt(111) and a Rh(100) crystal. The experiments on these reference samples were performed with an identical incident ion beam in order to have equal conditions and an equal number of incident ions at each reference sample. The error in the calibration can be ignored with respect to the measuring error in the actual experiments. This calibration revealed a sensitivity factor of 1.46 of Rhodium with respect to Platinum. The concentration of Platinum, C_{Pt}, is now calculated with:

$$C_{Pt}(atomic\_\%) = \frac{Yield(Platina)}{Yield(Rhodium) \times 1.46 + Yield(Platina)} \times 100. \qquad (12)$$

Before these experiments the surface composition was measured immediately after sputtering without flashing and this indeed revealed a surface composition of 50 % Platinum and 50 % Rhodium.

Results and discussion.

The results of the experiments are shown with the dots in Figure 4.1, where the concentration of Platinum is given in atomic percentage as a function of temperature. Also shown as the triangles are the results obtained by Moest et al [Barry] from a $Pt_{25}Rh_{75}$ (410) crystal.

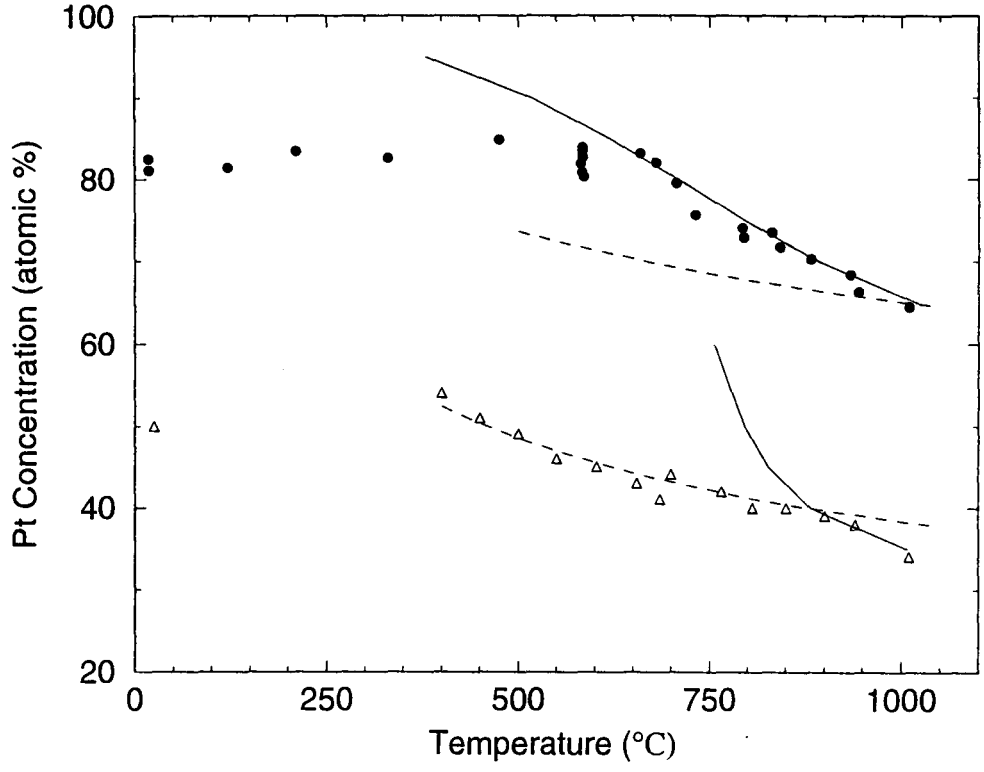

Figure 4.1 The surface concentration of Platinum as a function of temperature of the $Pt_{50}Rh_{50}$(611) crystal (•) and the $Pt_{25}Rh_{75}$ (410) crystal (Δ). Also shown are the corresponding fits which are clarified in the text.

What can be seen in Figure 4.1 is that in our experiments the concentration of Platinum stays reasonably constant at about 83 % until 500 degrees Celsius and than decreases to 65 % at 1000 degrees Celsius.

This indicates that the surface is not in equilibrium at temperatures ranging from room temperature to 500 degrees Celsius. When the crystal is flashed and than cools down to the desired temperature, the concentration of Platinum follows the ascending line. But at a certain temperature the surface "freezes" and the mobility of the atoms is too small to reach equilibrium.

These results are in accordance with the results obtained by Florencio et al [7], who found a Platinum concentration of 80 % of the surface layer at 700 degrees Celsius of a $Pt_{45}Rh_{55}$ (001) crystal.

The spread at higher temperatures can probably be explained with the error in temperature measurement (50 degrees Celsius). This error in the temperature gives, due to steep slope of the curve, rise to an error of 3 % in the concentration.

From Figure 4.1 it could be furthermore expected that the concentration at even higher temperatures decreases to the bulk value of 50 %. Due to the danger of melting of the surface layer at even higher temperatures this assumption was not verified. The experiments done by Moest et al [5] on a $Pt_{25}Rh_{75}$(410) crystal, shown as the triangles

in Figure 4.1, show that the Platinum concentration decreases to a value of 35 %. This value also approaches the bulk value of 25 %. This assumption is furthermore confirmed by Siera et al [4] who found a Platinum concentration of 25 % of a $Pt_{25}Rh_{75}(111)$ crystal at 1000 degrees Celsius.

The results shown could indicate either a zero or a non zero interaction coefficient as described in section 2.2.
The segregation energy in the case of a zero interaction coefficient can also be approximated with the broken bond model when only nearest neighbour interactions are considered. Moest et all [5] fitted their experiments with a ΔH_{sub} of 18 kJ/mol. This fit is shown in Figure 4.1 as the dashed line. Also shown in Figure 4.1 with the dashed line is the corresponding fit for our crystal with this ΔH_{sub} of 18 kJ/mol. In these fits it is taken into account that the surface composition is determined by a combination of the terrace and the step-edge atoms. It can be seen that this broken bond model does not fit the obtained experimental data contrary to the results of Moest et all.
The fitted line is not steep enough and as can be seen in section 2.3 this could indicate a non zero interaction coefficient. The dotted line shows the best fit for our results. This yields a ΔG of 2 kJ/mol and an interaction coefficient Ω of 15.5 kJ/mol. Also shown with a solid line is this fit applied to the experiments of Moest et al. It is very obvious that the solid line does not fit to the data. A larger interaction coefficient than the segregation energy is also not what is expected since Platinum and Rhodium have similar properties. This large interaction coefficient is therefore surprising.
There have to be done more experiments on other structures and more theoretical research has to be done in order to explain this behaviour.

The Platinum enrichment at the surface when the surface free energies are looked upon. The surface energies of Platinum and Rhodium calculated by Skriver et al[12] are given in Table 1.

Crystal	Surface energy (J/m^2)	Crystal	Surface energy (J/m^2)
Rh(100)	2.78	Pt(100)	2.35
Rh(111)	2.90	Pt(111)	2.48

Table 1 Surface free energies.

The surface energy of Platinum is lower than the surface energy of Rhodium. This explains why Platinum segregates to the surface.

The freezing process implicates that at a temperature around 600 degrees Celsius, when the atoms are not mobile enough to reach equilibrium while the temperature is decreasing but still posses mobility, the Platinum concentration would rise as a function of time after freezing.
The experiments done to verify this are described in the next section.

4.2.2 Segregation kinetics.

Experimental.

In this section the mobility of the atoms at 580 degrees Celsius is investigated in order to gain insight in the "freezing" process. This temperature is chosen because in Figure 4.1 it can be seen that this temperature is around the critical "freezing temperature". During these experiments the crystal was repeatedly sputtered and flashed three times before each measurement. After the last flash the crystal cooled down and kept at the desired temperature of 580 degrees Celsius. To obtain the same cooling down process for the different experiments the exact same settings for the oven where used, rather then using the pyrometer to adjust the temperature. The temperature indicated by the pyrometer was only used as an indication for the temperature. The indicated time is the time between the moment that the temperature indicated by the pyrometer remained constant and the moment at which the actual experiment took place. In the experiments after 12 and 20 minutes only 2 spectra where taken. This gives worse statistics but was necessary in order to minimize the error in the time determination since each spectrum takes about 1.5 minute. In the experiments after 40 minutes and longer 3 spectra where taken again.

Results and discussion.

The results are shown in Figure 4.2, where the concentration of Platinum is given as a function of time.

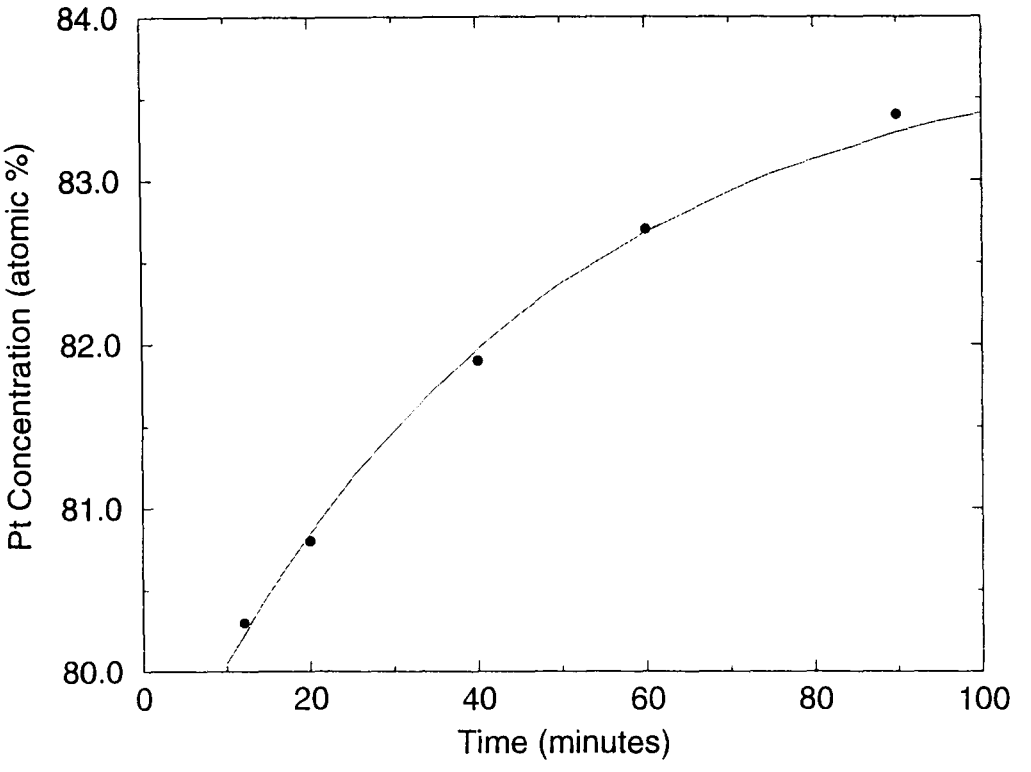

Figure 4.2 The surface concentration of Platinum as a function of time at 580 degrees Celsius (•) with the corresponding fit (solid line).

As can be seen in Figure 4.2 the concentration rises up to about 83.5 %. This confirms the assumption that the mobility of the atoms is not high enough to reach equilibrium while the crystal is cooling down, but when the temperature of 580 degrees Celsius is maintained the atoms are still mobile enough to reach equilibrium. Not shown in this graph is the experiment done after 15 hours. This experiment resulted in a concentration of Platinum of 84 %. This is consistent with the results shown in Figure 4.2.

At elevated temperatures Rhodium segregates to the surface. When the temperature decreases after flashing the Rhodium at the surface desegregates into the bulk. This desegregation can be described with a first order reaction, i.e. the rate of decrease in the Rhodium concentration at the surface dC/dt is proportional to the instantaneous Rhodium concentration at the surface C:

$$\frac{dC}{dt} = -kC, \tag{13}$$

were k is the rate of desegregation of Rhodium into the bulk.
For a concentration C_0 at an arbitrary time t = 0 this integration yields

$$C = C_0 \exp(-kt). \tag{14}$$

The Platinum concentration C_{Pt} (including the measurement after 15 hours) as a function of time can therefore be described by:

$$C_{Pt}(atomic\_\%) = 83.9 - C_0 \cdot \exp(-k \cdot t). \tag{15}$$

The factor 83.9 is the equilibrium Platinum concentration at this temperature as can be seen in Figure 4.2.
This fit yields C_0 = 4.84 % and k = 0.023 s^{-1}.

4.3 Backward TOF experiments.

4.3.1 Introduction.

In this section the experiments performed in order to find the step-edge concentration as a function of temperature are discussed. These experiments are done by using the backward TOF.
The step-direction has first to be determined. These experiments are discussed in paragraph 4.3.2. In paragraphs 4.3.3 and 4.3.4 the experiments are described to determine the step-up direction and possibly the angle of incidence needed for step-focusing. In paragraph 4.3.5 the actual step-edge measurements are discussed.

4.3.2 Azimuth scan in the horizontal plane.

Experimental.
In order to measure the step-edge concentration first the step direction has to be determined. The crystal is symmetric around the axis perpendicular to the steps. When an azimuth scan is made with the backward TOF the yield in either peak must also be symmetric around this axis.
These experiments where done with backward TOF. The used ions were 4 KeV Ne^+ ions which ensures good mass separation together with a good detector efficiency. The sample was sputtered and flashed three times before the experiment took place. The sample was turned in the horizontal direction over 360 degrees, where a spectrum was taken at every degree in the horizontal plane. In the resulting 360 spectra the total yield in the two peaks is accumulated at every degree. This is done by a program which simply adds all the counts in an arbitrary energy region.

Results and discussion.
The output of the fit program can be seen in Figure 4.3, where the total yield in the two peaks together is shown as a function of degrees in the horizontal plane.
The changing total yield can be explained with different shadowing effects in different crystal directions. In certain directions the surface atoms lie in the shadow cones of each other and this means a decrease in total yield.
In Figure 4.3 it can be seen that the graph is symmetric around two directions. Those two directions are at 141 degrees and 326 degrees (the positions of the dotted lines). The graph should be symmetric in the [110] and the $[\bar{1}\bar{1}0]$ direction as shown in Figure 3.7. These two directions should be 180 degrees apart, instead of the measured 326 minus 141 = 185 degrees. This can be explained with a bad calibration of the manipulator in this direction
(see Appendix A).

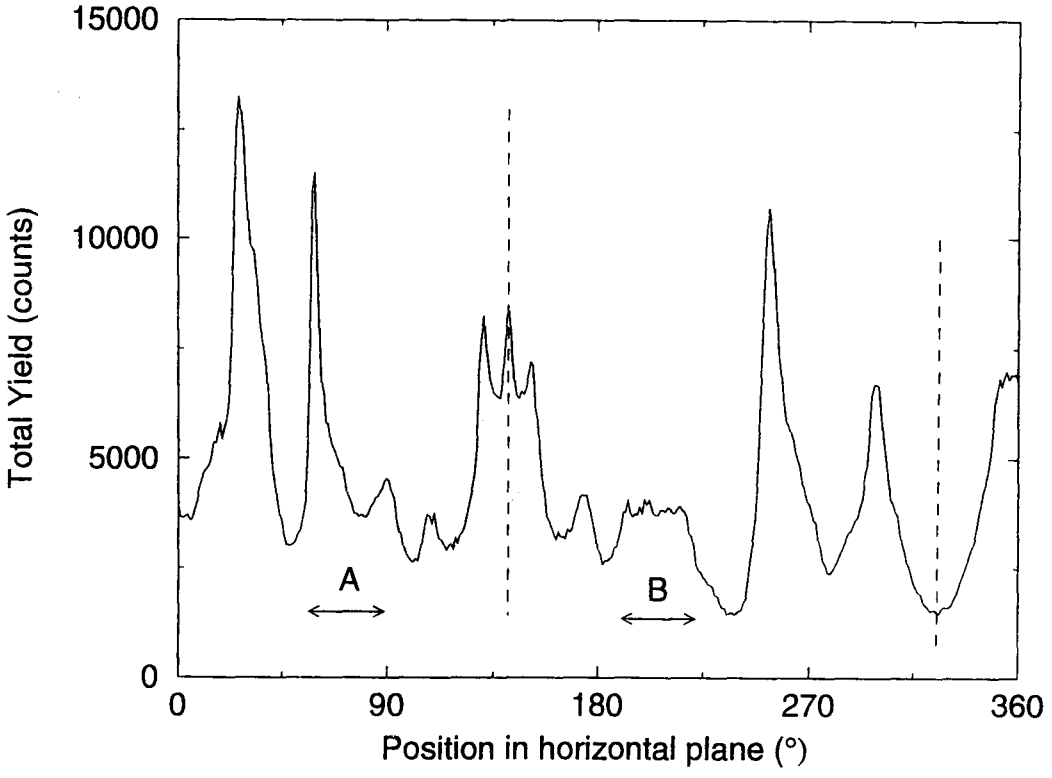

Figure 4.3 The total yield as a function of degrees in the horizontal plane.

The graph is symmetric when one pays attention to not only the position of the peaks but also to the slopes of the peaks. There are two regions however which are not symmetric. Those are region A compared with region B. The two peaks at 65 and 90 degrees in region A seem to disappear in region B. These regions were even larger in earlier experiments. By changing the position of the crystal with respect to the incident ion beam the regions were minimal in size at the current position. That there still is a non-symmetric region can probably explained with the sensitivity of the Time-Of-Flight technique. When the incident ion beam for instance is not exactly focused, the result could be a totally unfocused beam resulting in a large decrease in total yield. This could be caused by a not ideally horizontal positioned surface with respect to the incident ion beam. Another thought could be that the configuration of the sample could influence the total yield when the incoming beam is blocked by, for example, the sampleholder. This was found to be not probable because when the configuration of the sample was changed the non-symmetric regions still existed.
The step direction has now been determined but in order to measure the step-edge composition it is also necessary to determine the [1 1 0] and the $[\overline{1}\,1\,0]$ direction and possibly find the angle of incidence needed for step focusing as described in section 2.1.3.
These experiments are described in the next section.

4.3.2 Varying the incident angle at 141 degrees.

Experimental.

When the angle of incidence in backward TOF is varied it is possible to see focusing effects when the yield in either peak is shown as a function of angle of incidence. From the angle of incidence and the related focusing effects it is maybe possible to extract the angle of incidence when the incoming ions scatter from step-edge sites. In these experiments the incident angle of the ion beam was varied between 7 and 50 degrees. The sample was placed at 141 degrees in the horizontal plane. The crystal was sputtered and flashed three times prior to the experiments. The experiments are carried out at room temperature. At every degree a TOF Backward spectrum is obtained. In the acquired spectra the peaks are fitted with a Gauss. The yield in this peak is a measure for the ions scattered in binary collisions. A demonstration of this fit program can be seen in Appendix B.

The output of the program is the yield in the Gauss peaks as a function of degrees, since only the ions scattered through binary collisions are an indication for the concentrations at the surface.

Also in the TOF experiments the sensitivity of the detector, which is different for different elements, has to be taken into account. From previous experiments on PtRh crystals with 4 keV Ne^+ ions it is known that the sensitivity of Rhodium is 2.8 with respect to Platinum.

The Platinum concentration C_{pt} in atomic percentage is calculated in the following way:

$$C_{Pt}(atomic\_\%) = \frac{Yield(Platinum)}{Yield(Platinum) + 2.8 \times Yield(Rhodium)} \times 100. \qquad (16)$$

Due to the (611) structure of the crystal, as shown in Figure 4.4, the second layer is also visible to the incident beam, and therefore contributes to the measured concentration.

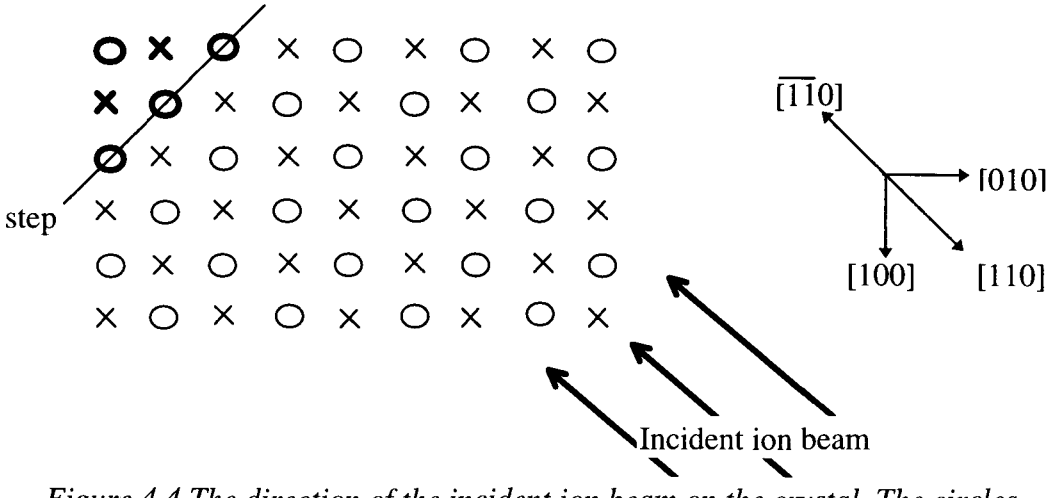

Figure 4.4 The direction of the incident ion beam on the crystal. The circles represent the first layer atoms, the crosses the second layer atoms.

From these experiments the Platinum concentration can also be calculated and from this the concentration the contribution of the second layer can be determined, since it is known from Florencio et al [7] that the Platinum concentration of the second layer is 30 %.

Simulations.

In Figure 4.5 mirror reflection, the slide effect and neighbour focusing are demonstrated by using a simulation program. It was not possible in this simulation program to create the (611) surface.

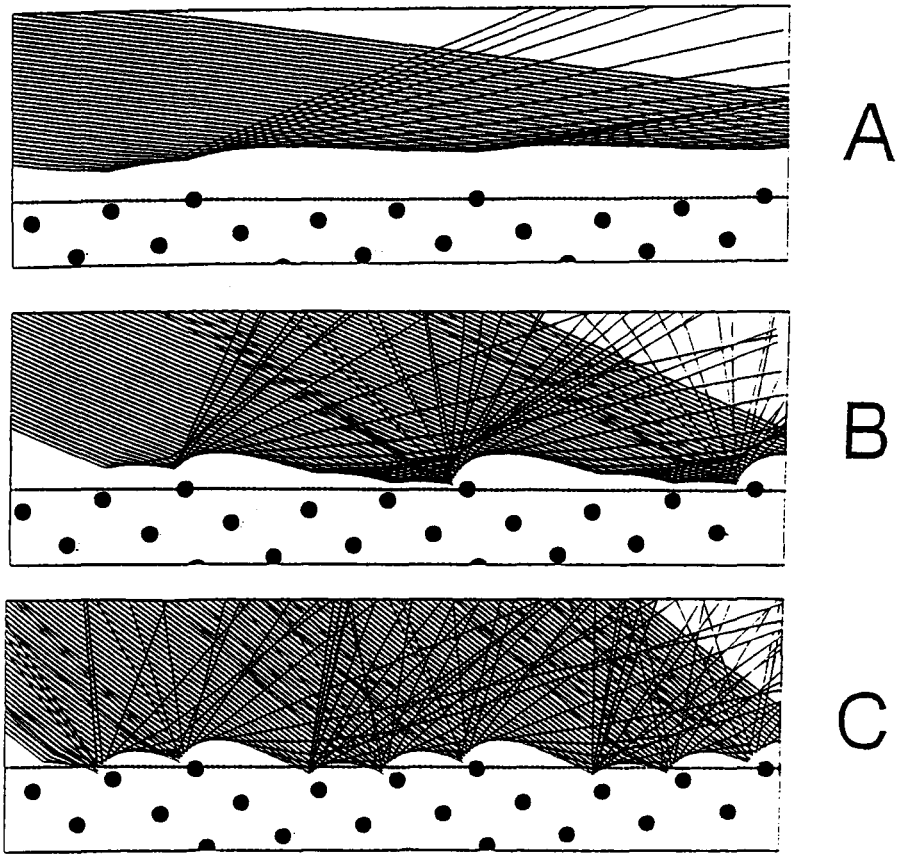

Figure 4.5 Examples of mirror reflection (a), slide effect (b) and neighbour focusing (c) created by using a 2 dimensional simulation program.

Results and discussion.

The results can be seen in Figure 4.6, where the Platinum and Rhodium yield are shown as function of the incident angle of the ion beam.

The decrease in yield below 15 degrees is due to the fact that the incident ions are in the mirror reflection mode and are not able anymore to reach the detector (see Figure 4.5a).

The maximum at 23 degrees in Figure 4.6 is due to neighbour focussing (see Figure 4.5c).

In the range between 28 degrees and 45 degrees the incident ion beam is in the unfocused mode. This means that every site will receive the same ion-flux and thus will the ion beam "see" every site equally.

At 45 degrees the signal starts rising again which is probably due to focussing on the second layer. According to experiments done by Florencio et al [7] this layer should be Rhodium enriched. Unfortunately the setup does not allow measurements at larger angles of incidence.
The peak of the Rhodium signal is not in the same place as the peak of the Platinum signal. This is due to the fact that the impact parameter in neighbour focusing of Rhodium is smaller than the impact parameter of Platinum. This results in a larger angle of incidence needed for neighbour focusing for Rhodium.

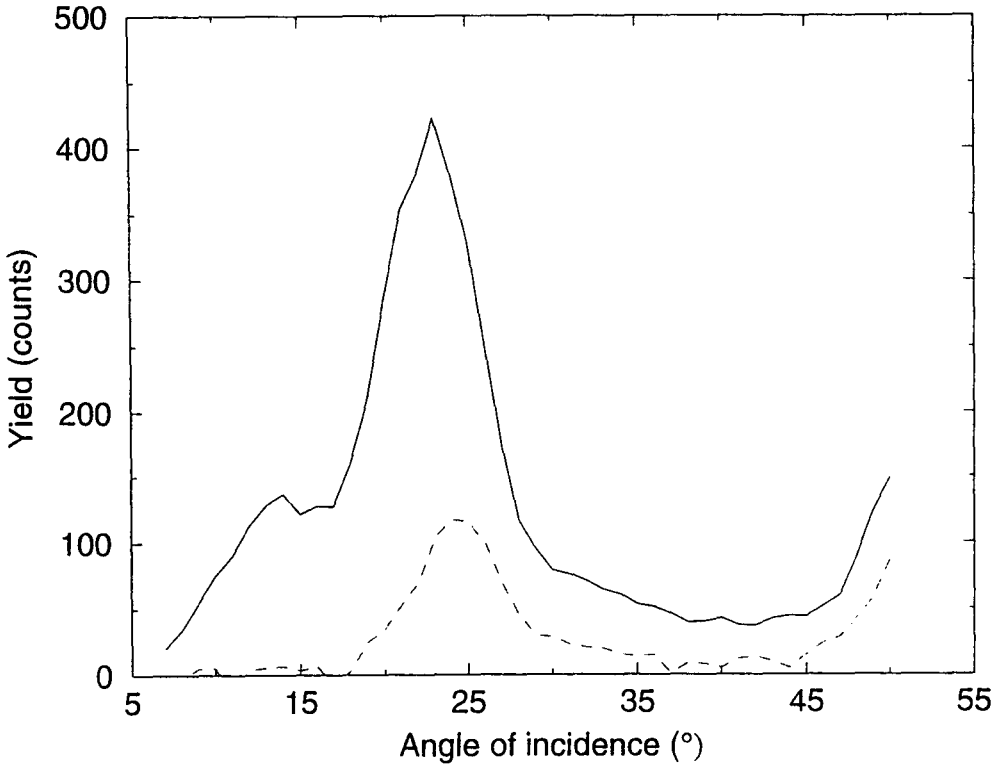

Figure 4.6 The Platinum (solid line) and Rhodium (dashed line) yield as a function of incident angle.

The Platinum concentration, with correction for the sensitivity, as a function of incident angle is given in Figure 4.7.
There are several interesting aspects in this Figure 4.7.
In paragraph 4.3.4 it will be determined that this direction at 141 degrees is the step-down direction. This explains the value of concentration between angles of incidence ranging from 13 to 17 degrees. In this range the ions scatter from the step-edges and from terrace atoms near the step-edge. The height of this plateau in comparison with the rest of the graph is a first indication that the step-edges contain more Platinum, because relatively more step-edge sites are measured than at larger angles of incidence. This is also already seen by Moest et all on a PtRh(410) crystal [5].
The concentration then drops to a value of 45 % at an angle of incidence of 26 degrees. This is caused by neighbour focusing.

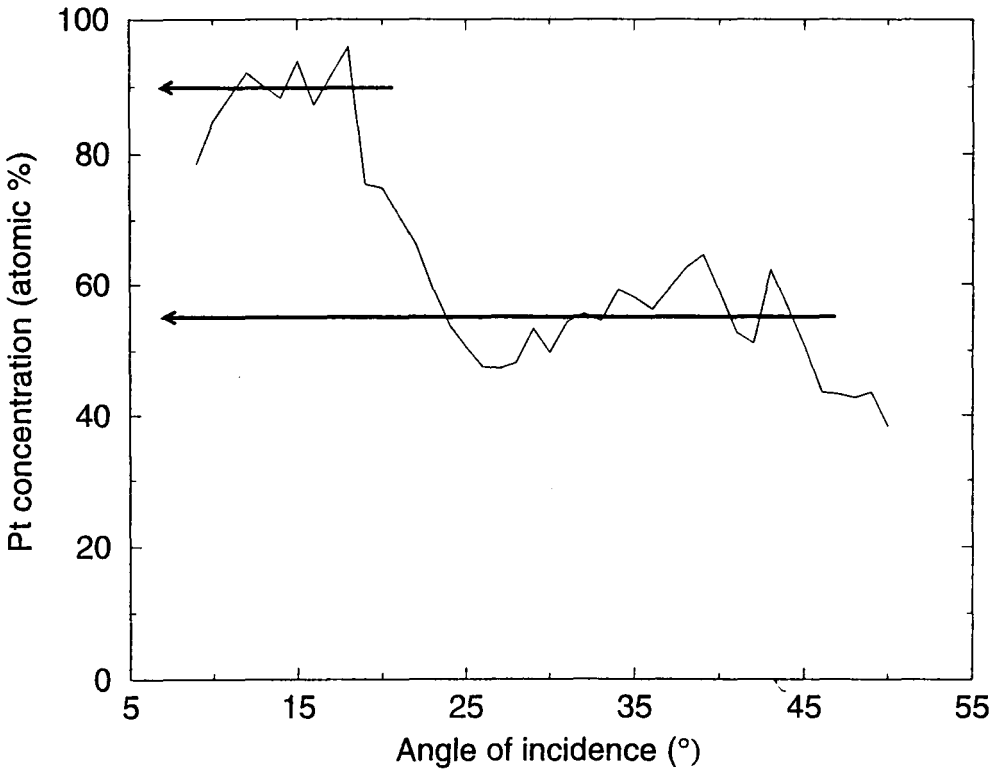

Figure 4.7 The Platinum concentration with correction for the sensitivity as a function of incident angle at 141 degrees.

There is another plateau between 30 and 40 degrees at a value of 55 %. This plateau is due to the fact that at these angles of incidence the incident ion beam is in the unfocused mode. This plateau is not at the same height as the minimum at 26 degrees. This is caused by the fact that in neighbour focusing not every site, for instance a step-edge site and a terrace site, is seen equally by the detector.
From this plateau at 55 % it is possible to calculate the yield coming from the second layer with:

$$55\% = \varepsilon \times 83\% + (1-\varepsilon) \times 30\%, \qquad (17)$$

where 55 % is the height from the plateau, 83 % the Platinum concentration as measured in section 4.2, 30 % the Platinum concentration in the second layer as found in experiments done by Florencio et al [7] on a $Pt_{50}Rh_{50}$ (001) crystal and ε the percentage of ions scattered from the first layer.
This yields ε = 47 %. So half of the detected ions are scattered from the first layer and the other half from the second layer.
The Platinum concentration than decreases further to a value of about 40 %. At these larger angles of incidence incoming ions are getting focused on the second layer and this layer is Rhodium enriched as mentioned earlier. Therefore the Platinum concentration decreases.

In these experiments step-focusing can not be seen. The only way to determine the step-edge concentration is by using the "slide" effect as shown in Figure 4.5b. The incoming ions slide over the surface and scatter from either the step-edges or surface defects. In order to determine the step-up direction the same experiments have been done in the direction at 326 degrees.

4.3.4 Varying the incident angle at 326 degrees.

Experimental.
In this section the experiments are described which were done in order to determine the step-up direction.
In these experiments the same conditions were used as described in section 4.3.2. Now the crystal is turned to the position of 326 degrees. The obtained spectra were analyzed with the same fit program used in paragraph 4.3.2.

Results and discussion.
The results can be seen in Figure 4.8, where the total yields of Rhodium and Platinum are given as a function of angle of incidence of the ion beam.

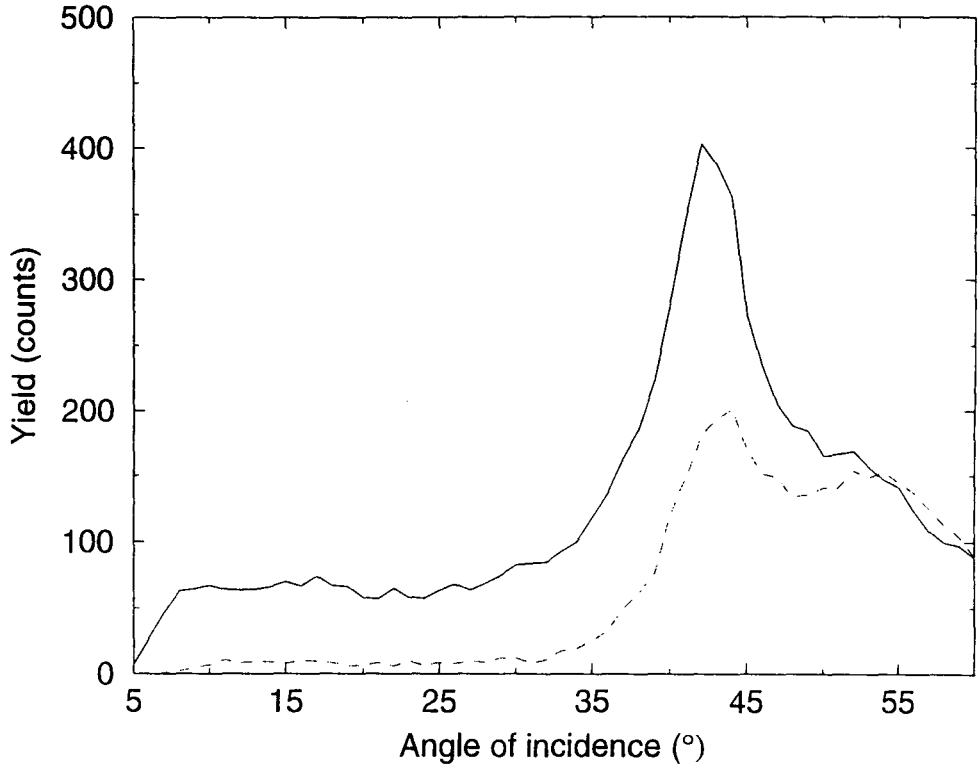

Figure 4.8 Yield of Platinum (solid line) and Rhodium (dashed line) as a function of angle of incidence at 326 degrees.

In this figure can be seen that the decrease at low angles of incidence, due to the mirror reflection mode, occurs again at angles of incidence lower than 9 degrees. At higher angles of incidence, up to 32 degrees, the incoming ions "slide" over the surface due to the potentials of the surface atoms. This implicates that the incoming atoms slide over the surface and than scatter of either a step-edge atom or a defect. The peak at 42 degrees can be subscribed to neighbour focussing. The effect of step focussing again can not be seen in these experiments.
The small peak at 52 degrees in the Rhodium concentration is probably due to focusing on the second layer which is Rhodium enriched as mentioned earlier.

When Figure 4.8 is compared with Figure 4.6 it can be seen that the peak of the neighbour focussing in Figure 4.6 lies at an incident angle of 23 degrees, while in Figure 4.8 this peak lies at an incident angle of 42 degrees. This difference can be explained with the configuration of the surface as shown in Figure 4.9.

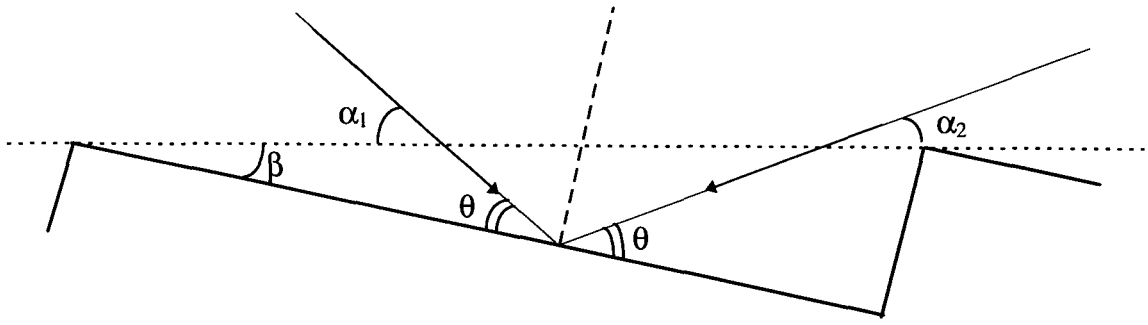

Figure 4.9 Schematic representation of the surface.

In Figure 4.9 θ is the angle of incidence needed for neighbour focusing. This leads to the angles α_1 and α_2 which are the angles of incidence as measured in these experiments.
From the difference in the angle of incidence which causes neighbour focusing it can be concluded that the angle β, the miscut of the crystal, is about 10 degrees as shown in Figure 4.9. The miscut of a (611) crystal is 13 degrees. This difference can be explained with a not ideally horizontal positioned sample. It could be caused by a tilt of 0.4 mm. on one side of the crystal which is 7 mm. in diameter. This is not unlikely in the used setup.
For the step-up direction the neighbour focusing occurs at a larger angle of incidence then for the step-down direction as can be seen in Figure 4.9 ($\alpha_1 > \alpha_2$). From this it can be concluded that the $[\bar{1}10]$ direction is indeed positioned at the angle of 326 degrees in the horizontal plane (neighbour focussing at 42 degrees), while the [110] direction is positioned at an angle of 141 degrees in the horizontal plane (neighbour focussing at 23 degrees).

In figure 4.10 the Platinum concentration with correction for the sensitivity of the detector is shown.
The "slide" effect as described on the previous page implicates that in the range from 10 degrees up to 32 degrees the concentration should remain constant, because in this range the measured concentration equals the step-edge concentration. As can be seen in Figure 4.10 this is indeed the case.
There is no plateau at the position of the neighbour focussing. An explanation is that the peak is too small to have a plateau in the concentration profile and because the concentration keeps decreasing this particular plateau can not be distinguished, contrary to the step-down direction where this plateau is a local minimum.

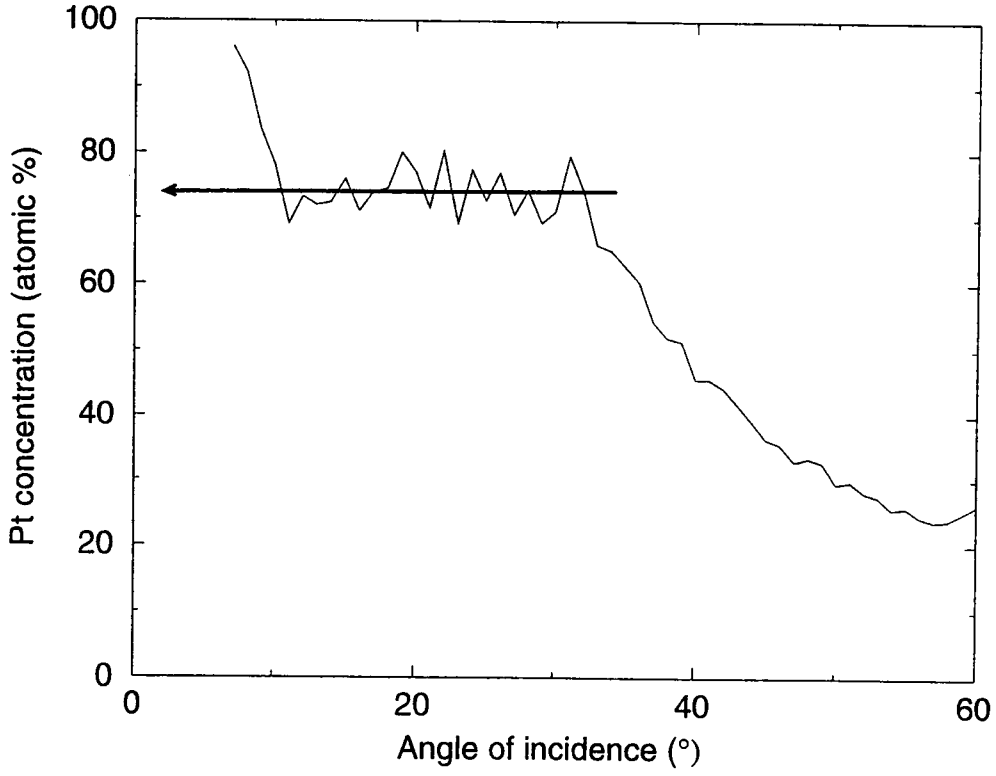

Figure 4.10 The Platinum concentration with correction for the sensitivity as a function of incident angle at 326 degrees.

4.3.5 Step-edge concentration as a function of temperature.

Experiments.

In the previous sections it was concluded that the position of 326 degrees in the horizontal plane is the $[\bar{1}10]$ direction. It was also seen that in this direction the incoming ions "slide" over the surface and scatter not only from the step-edge atoms in the range of 15 to 32 degrees, but also from the atoms in the second layer of the step.

In order to investigate the step-edge concentration this direction of 326 degrees in the horizontal plane and an angle of incidence of 20 degrees are used.

The Platinum concentration is calculated according to formula (16) in paragraph 4.3.2.

The crystal is sputtered regularly and is flashed three times before each measurement. After the last flash the sample is cooled down to the desired temperature. At this temperature the crystal is given 60 to 90 minutes to reach equilibrium.

Results and discussion.

The results are shown with the dots in Figure 4.11. Also shown in Figure 4.11 with the triangles are the results obtained by Moest et al [5] on a $Pt_{25}Rh_{75}(410)$ crystal.

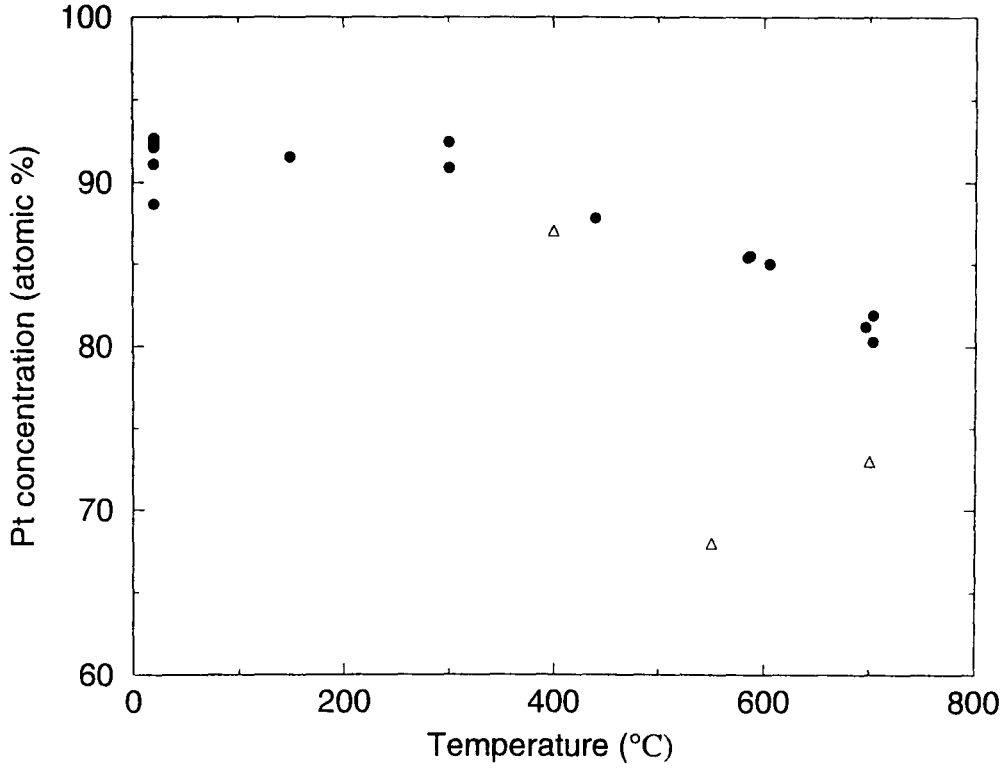

Figure 4.11 The Platinum concentration in the step edges as a function of temperature for the $Pt_{50}Rh_{50}(611)$ crystal (•) and a $Pt_{25}Rh_{75}(410)$ crystal (Δ).

In Figure 4.11 it can be seen that up to 300 degrees Celsius the Platinum concentration stays constant at around 90 %. After 440 degrees Celsius the concentration drops to 82 % at 700 degrees Celsius. This concentration is a lower limit to the real step-edge composition, as not 100 % scatters from the step-edges. When is assumed that 50 % scatters from the sites below the step-edge sites and that the composition of these sites equals the terrace composition of 80 %, the actual step-edge concentration at room temperature would be 95 %.
In comparison with the surface concentration of Platinum as measured in section 4.2, the step-edge concentration of Platinum is significantly higher. This is in accordance with the results from Moest et al [5] and Wouda et al [6]. They also find a higher Platinum concentration at the step-edges.
These results can not be fitted because of the upper limit in temperature of 700 degrees Celsius. This upper limit is due to the fact that the Time-Of-Flight detector is not able to measure when e-beam heating is used. Without this e-beam heating the crystal can only be heated up to 700 degrees Celsius.

4.4 Introductory absorption experiments.

Experiments.
In this section the introductory experiments investigating the absorption of Oxygen and the influence of this absorption on the surface composition are described. This is very interesting from a catalytic point of view.
The crystal was sputtered regularly and flashed three times prior to all the experiments.
The experiments were done with the EARISS detector and 2 keV He^+ ions. The incident ion beam is approximately identical in the different experiments.
The results are shown in Figure 4.12.

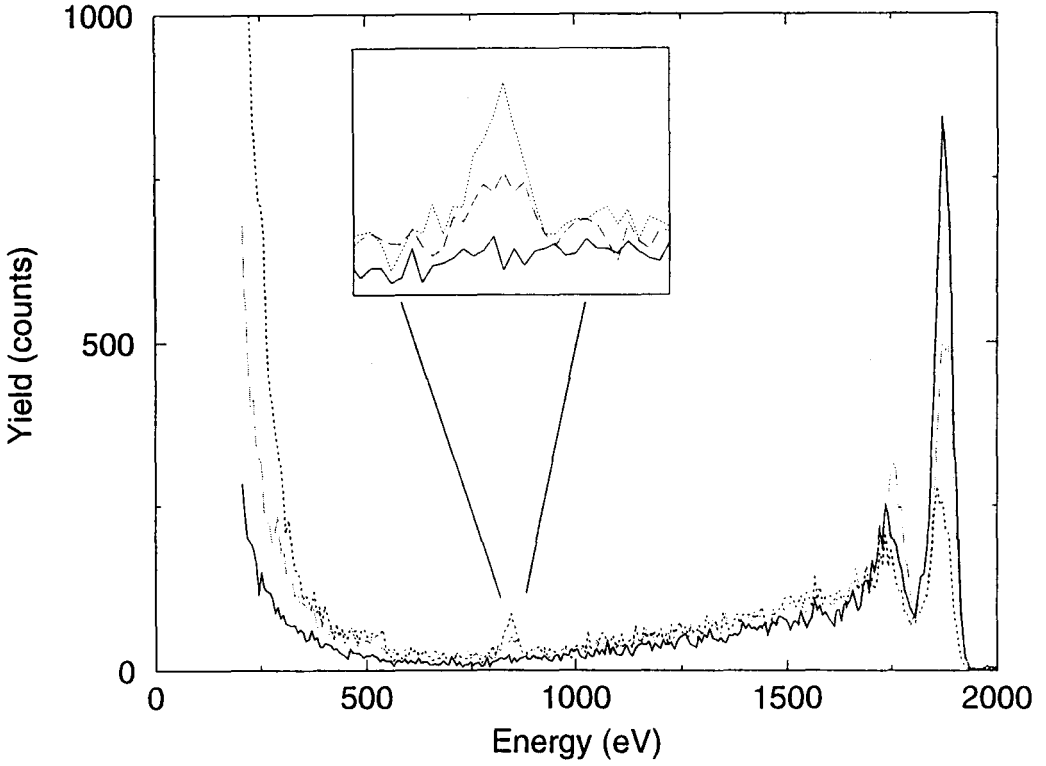

Figure 4.12 TOF-Backward spectra obtained after in chronological order: flashing (solid line), treatment with $2 \cdot 10^{-7}$ mbar O_2 during 45 minutes (dotted line) and treatment with $3 \cdot 10^{-7}$ mbar H_2 during 30 minutes (dashed line).

First a spectrum of the crystal prior to Oxygen treatment was taken. This is shown in Figure 4.12 as the solid line.
The crystal was then exposed to Oxygen during 45 minutes with a pressure of $3 \cdot 10^{-7}$ mbar. The spectrum was taken after the Oxygen was removed from the vacuum chamber. This spectrum is shown in Figure 4.12 as the dotted line. It can be seen that there is a peak at about 800 eV. The calculated Oxygen peak with 2 keV He^+ is situated at 788 eV, so it can be concluded that Oxygen is absorbed on the surface. Furthermore the peaks of Rhodium (left peak) and Platinum (right peak) decrease in height. The Rhodium peak decreases less than the Platinum peak. This could be due to Rhodium segregation but it is also possible that Oxygen preferentially absorbs on

Platinum and thereby decreases the Platinum signal. According to van Delft [10] Oxygen absorbs preferentially on Rhodium instead of on Platinum.
When it would be possible to remove the Oxygen at low temperatures the real surface composition can be obtained and also could be determined if Oxygen absorbs preferentially, for at low temperatures the mobility of the atoms is too low to reach equilibrium.
Therefore the crystal is exposed at room temperature to Hydrogen during 30 minutes with a pressure of $2 \cdot 10^{-7}$ mbar. This is shown in Figure 4.12 as the dashed line. The spectrum is taken after Hydrogen is removed from the vacuum chamber. It can be seen that indeed the yield in the Oxygen peak decreases with about 50 %. Both peaks increase but the Rhodium peak increases also with respect to the Platinum peak. From this it can be concluded that when Oxygen is absorbed on the surface Rhodium segregates to the surface. This is also seen in experiments done by Tamura et al [8], Matsumoto et al [9] and van Delft [10].

In future work it is recommendable to heat the sample to a temperature of, for instance 200 degrees Celsius, when the crystal is exposed to Hydrogen. At these temperatures the Oxygen is expected to be removed from the surface more easily, while the mobility of the atoms is too small to have a change in surface composition, as can be concluded from the EARISS experiments in section 4.2.

Chapter 5 Conclusions.

The Platinum concentration of a $Pt_{50}Rh_{50}$ (811) crystal at room temperature is 83 ± 3 %. This is in accordance with experiments done by Florencio et al [7]. When the crystal is heated this concentration remains constant up to 600 degrees Celsius and then decreases to 65 % at 1000 degrees Celsius. The broken bond model can not explain this behaviour, contrary to the model with a non-zero interaction coefficient. The Platinum concentration of a $Pt_{25}Rh_{75}$ (410) crystal can however be well described with the broken bond model. Therefore more experiments have to be done to explain this different behaviour.
The Platinum enrichment at the surface can be understood when the surface free energies are looked upon. The surface energies of Platinum and Rhodium calculated by Skriver et al[12] are given in Table 1.

Crystal	Surface energy (J/m^2)	Crystal	Surface energy (J/m^2)
Rh(100)	2.78	Pt(100)	2.35
Rh(111)	2.90	Pt(111)	2.48

Table 1 Surface free energies.

The surface energy of Platinum is lower than the surface energy of Rhodium. This explains the Platinum segregation.

When the crystal is flashed and cooled down to 580 degrees Celsius the time dependence of the Platinum concentration, C_{Pt}, in atomic percentage at this temperature can be expressed as:

$$C_{Pt}(atomic\_\%) = 83.9 - C_0 \exp(-kt).$$

where C_0 is an arbitrary constant and k is the rate of desegregation of Rhodium into the bulk. This fit yields $C_0 = 4.84$ % and $k = 0.023\ s^{-1}$.

The direction of the steps can be determined by performing an azimuth scan in the horizontal plane with Time-Of-Flight.
By varying the angle of incidence in the two directions perpendicular to the step direction the step-up and step-down direction can be distinguished.
No step focussing can be seen in these experiments, but by using small angles of incidence it is possible to measure the composition of the step-edge atoms as the incident ions "slide" over the surface and only scatter of the step atoms or defects.

The experiments show that the Platinum concentration at room temperature is in the range between 88 and 92 %. It remains constant up to 440 degrees Celsius and than decreases to 82 % at 700 degrees Celsius. This concentration is a lower limit to the real step-edge composition, since not all incoming ions scatter from the step-edges. When is assumed that 50 % scatters from the sites below the step-edge sites and that the composition of these sites equals the terrace composition of 80 %, the actual step-edge concentration at room temperature would be 95 %.
The enhanced Platinum segregation to the step-edges is in agreement with experiments done by Moest et al [5], which also show more Platinum enrichment in the step-edges of a PtRh(410) crystal.

The crystal has been exposed to Oxygen during 45 minutes with a pressure of $3 \cdot 10^{-7}$ mbar. From the EARISS experiments it can be seen that Oxygen is absorbed on the surface. The yield of both Rhodium and Platinum in the EARISS spectrum decrease. The Rhodium yield decreases less with respect to the Platinum yield. This could be due to Rhodium segregation but it is also possible that Oxygen preferentially absorbs on Platinum and thereby decreases the Platinum signal.
When it would be possible to remove the Oxygen at low temperatures the real surface composition can be obtained, for at low temperatures the mobility of the atoms is too low to reach equilibrium.
Therefore the crystal has been exposed at room temperature to Hydrogen during 30 minutes with a pressure of $2 \cdot 10^{-7}$ mbar. In the EARISS spectrum it can be seen that indeed the Oxygen yield decreases with 50 %. The Rhodium peak increases relatively to the Platinum peak. From this it can be concluded that when Oxygen is absorbed on the surface Rhodium segregates to the surface. This is also seen in experiments done by Tamura et al [8], Matsumoto et al [9] and van Delft [10] on PtRh crystals.
There have to be done more experiments investigating Oxygen absorption in order to gain more insight and to be able to quantify the effect of Rhodium segregation due to Oxygen absorption.
In future work it is recommendable to heat the sample to a temperature of, for instance 200 degrees Celsius, when the crystal is exposed to Hydrogen. At these temperatures the Oxygen is expected to be entirely removed from the surface, while the mobility of the atoms is too small to have a change in surface composition, as can be concluded from the EARISS experiments.

Appendix A.

The graph shown is obtained when the azimuth scan in the horizontal plane as shown in Figure 4.3 is folded around the symmetric point of 141 degrees.
It can be seen that the calibration of the step-motor drive is not correct and that the position of the corresponding peaks shift.

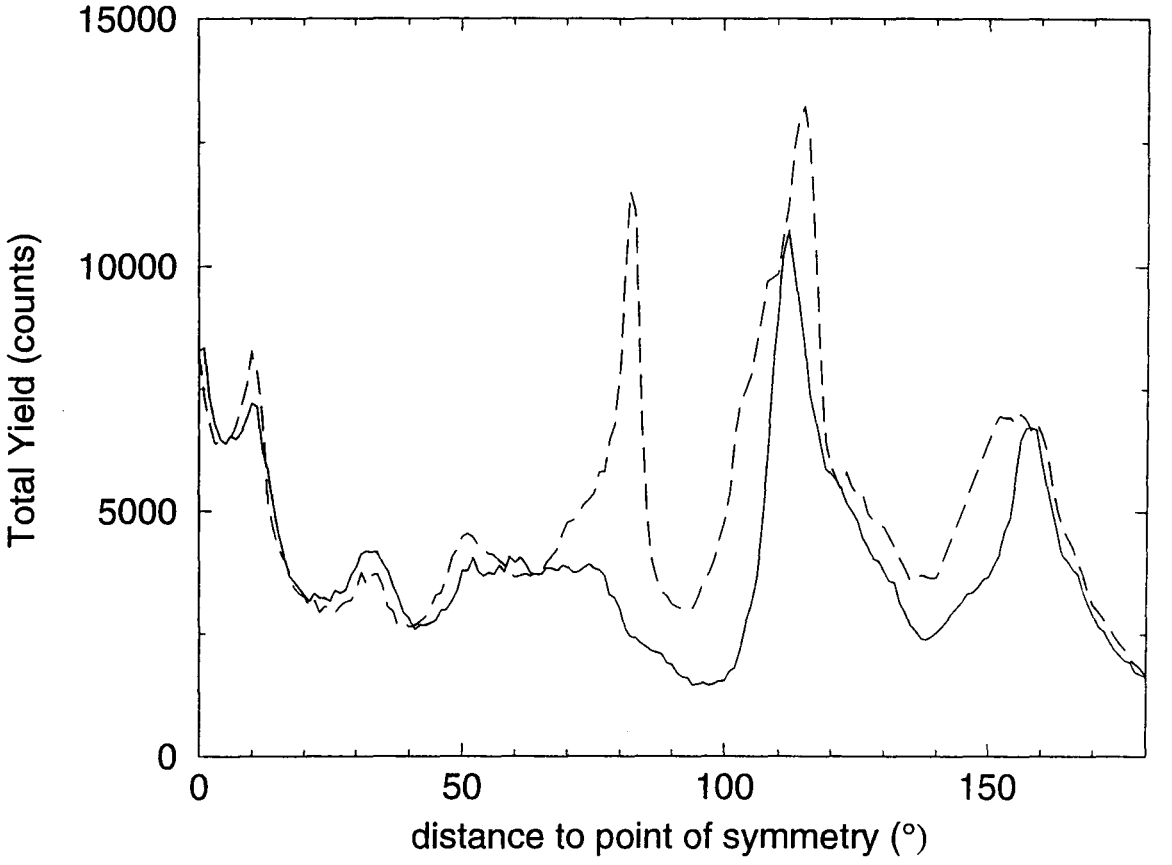

Appendix B.

In this figure a demonstration can be seen of the fit program used in analyzing the Time-Of-Flight spectra.
In the acquired spectra the peaks are fitted with a Gauss. The tail of the peak, which consists of ions multiply scattered, is fitted as a linear curve starting at zero at the position of the FWHM on the left hand side of the peak of the Gauss curve. It rises linear until the position of the FWHM on the right hand side. At that point the curve drops exponentially. The overall background is taken to be linear.

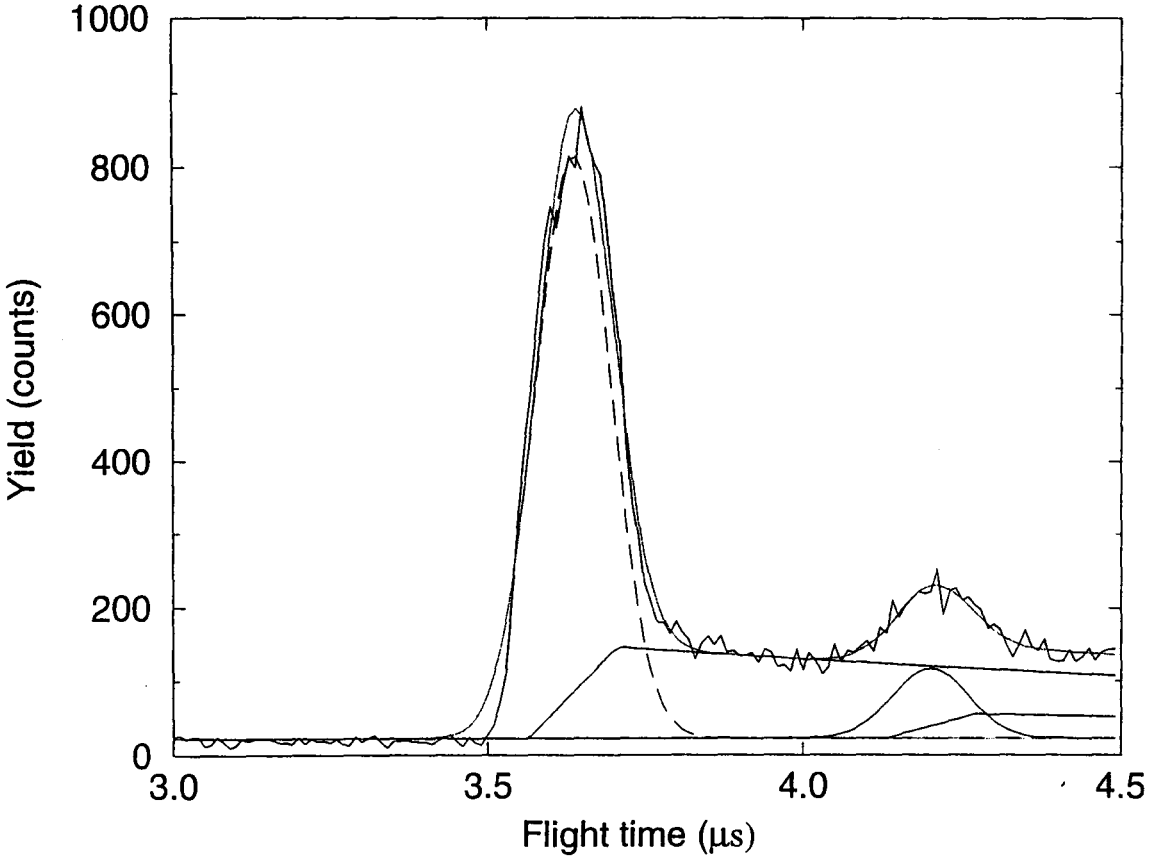

Appendix C.

This graph shows the total yield of the Time-Of-Flight detector as a function of time. It can be seen that the total yield drops with about 20 %. This is due to the stabilizing gas pressure in the ion source.
During long measurements this effect has to be taken into consideration.

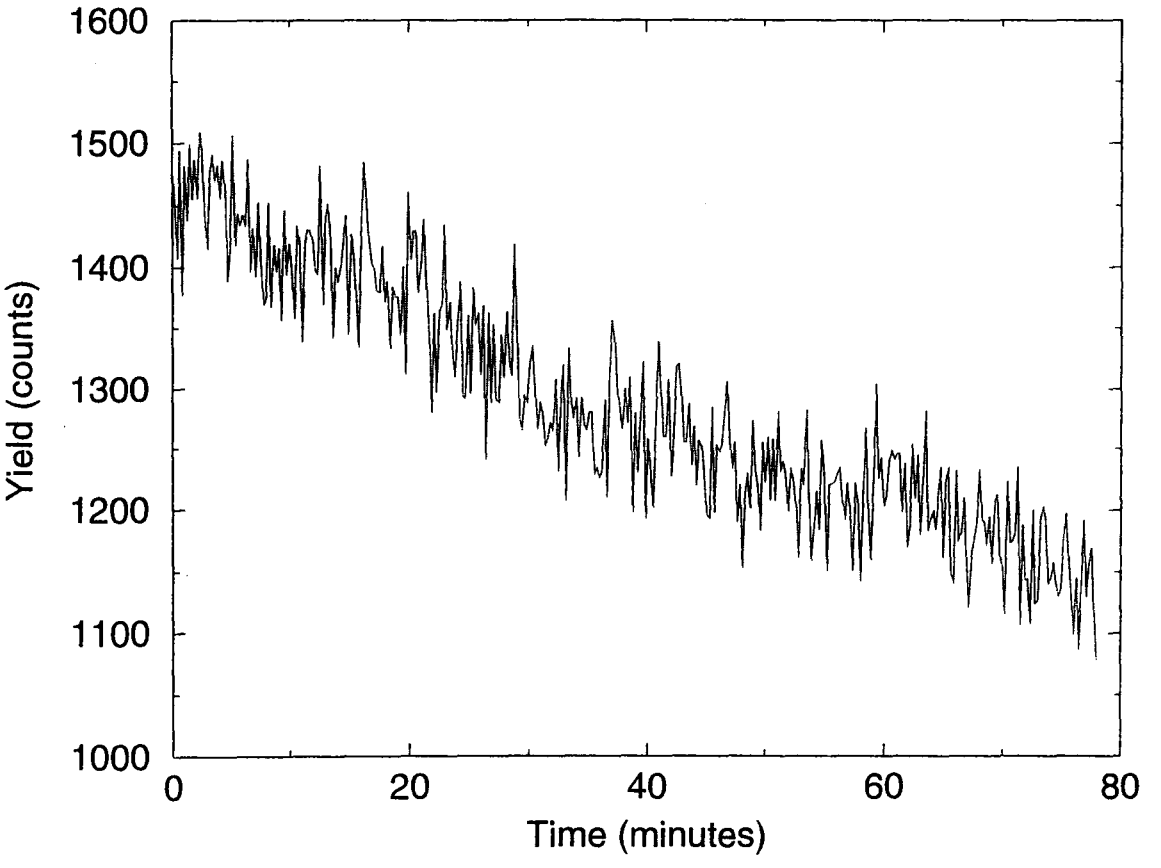

References.

[1] Atomic collisions on solid surfaces.
Parilis et al.
North Holland, 1993, 664

[2] Surface segregation.
J. du Plessis.
Sci-Tech Publications, 1990, 125

[3] Low Energy Electron Diffraction.
Pendry.
Academic Press,1974, 407

[4] The composition of the (111) and (100) surfaces of a $Pt_{25}Rh_{75}$ single crystal.
J. Siera et al.
Surface Science 264, 1992, 435-439

[5] Step-edge segregation of bimetallic alloys.
B. Moest et al.
to be published

[6] Chemically resolved STM on a PtRh(100) surface.
P.T. Wouda et al.
Surface Science 359, 1996, 17-22

[7] Absolute composition depth-profiles in surface segregation of Pt-Rh alloys.
J. Florencio et al.
Surface Science 345, 1996, L29-L33

[8] Activation of the Pt deposited Rh(100) bimetallic surface by chemical ordering.
H. Tamura et al.
Surface Science 303, 1994, L379-L384

[9] STM studies of a catalytically active p(3×1) Pt-Rh(100) alloy surface.
Y. Matsumoto et al.
Surface Science 355, 1996, 109-114

[10] The transient behaviour of Pt-Rh(410) alloy surfaces upon interaction with O_2, NO and CO.
F.C.M.J.M Van Delft.
Surface Science 208, 1989, 365-382

[11] Surface enrichment of $Pt_{10}Rh_{90}(111)$.
D.D. Beck et al.
Surface Science 359, 1993, 303-311

[12] Surface Energy and work function of elemental metals.
H.L. Skriver et al.
Physical Review 46-11, 1992, 7157-7168

Thank you.

I want to thank all the people at FOG who made this last year a fun year. Of course I want to thank Barry for "showing me the way" (never thought I would make it without being hit), Gerard for his technical support and "pump-lessons", Arnoud for asking me difficult questions after which I had to think very hard (nothing wrong with that) and Prof.Dr. Brongersma for letting me do this project in the FOG group.
Also I want to thank Rene for, uuuh, the delicious "worstebroodjes", Marco for all the conversations full of sorrow we had together and my Belgium friends "proud to be a Belgian"-Steve and "ge laat me schrikken"-Patricia for assisting me during the experiments.
Last but definitely not least I want to thank the EARISS for all the good and bad times we shared together. EARISS rules.
Of course there are a lot of people which I haven't mentioned here. To them I just wanna say: I know who you are and you know who you are. Thanks.

Take care.

Mischa.